6-1-2015

Metagenomic profiling of microbial metal interaction in Red Sea deep-anoxic brine pools

Mina Magdy Abdelsayed Hanna

The American University in Cairo

School of Sciences and Engineering

Metagenomic Profiling of Microbial Metal Interaction in Red Sea Deep-Anoxic Brine Pools

A Thesis Submitted to The Biotechnology Graduate Program in partial fulfillment of the requirements for the degree of Master of Science in Biotechnology

By

Mina Magdy Abdelsayed Hanna

Under the supervision of

Dr. Rania Siam

Associate Professor, Chair-Biology Department
The American University in Cairo

Spring 2015

The American University in Cairo

Metagenomic profiling of microbial metal interaction in Red Sea deep-anoxic brine pools

A Thesis Submitted by Mina Magdy Abdelsayed Hanna

To the Biotechnology Graduate Program

Spring 2015

In partial fulfillment of the requirements for the degree of Master of Science in Biotechnology

Has been approved by

Dr. Rania Siam

Thesis Committee Chair / Supervisor

Associate Professor and Chair, Biology Department, AUC

Dr. Ahmed Moustafa

Thesis Committee Internal Examiner

Associate Professor and Director, Biotechnology Graduate Program

Biology Department, AUC

Dr. Ramy Aziz

Thesis Committee External Examiner

Assistant Professor, Faculty of Pharmacy, Cairo University

Dr. Andreas Kakarougkas

Thesis Committee Moderator

Assistant Professor, Biology Department, AUC

_____	_____	_____	_____
Program Director	Date	Dean	Date

DEDICATION

This work is dedicated to my beloved mother and sister who always supported and encouraged me to fulfill my dreams and achieve more success in my life. This work is also dedicated to the soul of my father.

ACKNOWLEDGEMENTS

I would like to express gratitude to Dr. Rania Siam, Associate Professor, Chair-Biology Department, and advisor of this thesis for her thoughtfulness, continuous support, encouragement and contribution to this work. I would like to thank Dr. Hamza El Dorry, Professor, Biology Department, for sharing data. I would like to acknowledge Dr. Rania Siam, Dr. Ahmed A. Sayed, Dr. Mohamed Ghazy and Mr. Amged Ouf for doing sampling and DNA extraction work. Moreover, I would like to thank Mr. Mustafa Adel, bioinformatics analyst, for his support and help in computational analysis. Likewise, I would like to thank the faculty of Biotechnology Graduate Program in AUC, especially Dr. Ahmed Moustafa who taught me the fundamentals of bioinformatics. I would like to thank all my colleagues who helped and advised me while doing this work, specifically; Mr. Ali El Behery, Ghada Moustafa and Rehab Abdallah. Last but not least, I would like to thank Al Alfi Foundation for funding my MSc. studies, and King Abdullah University for Science and Technology (KAUST) for supporting this research.

Metagenomic Profiling of Microbial Metal Interaction in Red Sea Deep-Anoxic Brine Pools

ABSTRACT

Extreme environmental conditions induce evolution of microbiomes and shape microbial abundance. Different geochemical studies reported high metal abundance in Red Sea deep-anoxic brine pools, especially in Atlantis II Deep, which has the highest metals content. Brine pools show wide diversity of biologically essential and non-essential metals. Several metals known for their toxicity to biological life were detected in these pools. Yet, previous microbiome analyses of the pools demonstrated vast microbiological diversity. In this study, we compare metal-resistant prokaryotic microbiomes in different metal-rich brine water samples from Atlantis II lower convective layer (ATII-LCL), Atlantis II upper convective layer (ATII-UCL), Discovery Deep (DD) and Kebrit Deep (KD). Moreover, we investigate genome evolution of microbial communities in response to such excessive metal abundance. Using 16S rRNA pyrotags and shot-gun 454-pyrosequencing, we perform a comparative analyses of (i)-taxonomic assignment of operational taxonomic units to major bacterial and archaeal groups and (ii)-metal resistant protein-coding genes, of the microbial communities and metagenomes. The ATII-LCL, ATII-UCL, DD and KD brine pools metagenomes protein-coding genes involved in microbial-metal interaction and resistances were assessed for abundance and diversity. We report specific microbial richness of these three brine pools. Functional analyses of the metagenomes revealed different metal resistance mechanisms and different modes of mutual interaction between dissolved metals/sediments and microbial communities. This was supported by the strong correlation between specific high metal/s concentration in selected brine water, where; metal resistance, enrichment of metals metabolism and transport were revealed. As expected, ATII-LCL showed the highest relative abundance of genes involved in microbial-metal interaction. Additionally, we report significant abundance of peroxidases-encoding genes, mainly in ATII-LCL, and we hypothesize that generation of hydrogen peroxide (H_2O_2) occurs through interaction of pyrite deposits. Moreover, we suggest that genus *Paenibacillus*, which is highly abundant in ATII-LCL has a role in increasing concentration of dissolved iron in brine water. DD and KD showed relatively lower enrichment of genes involved in microbial-metal interaction. However, geochemistry of these environments together with unique microbial abundance give an inference about mechanisms of microbial metal interaction and metabolism taking place there. Eventually, we successfully identified free living metal-resistant prokaryotic communities, showed how prokaryotes tolerate and induce changes to the surrounding environment, and highlighted how geochemical conditions affected microbial abundance and induced evolution of microbiomes.

TABLE OF CONTENTS

LIST OF FIGURES

LIST OF TABLES

LIST OF ABBREVIATIONS

ATII	Atlantis II Deep
LCL	Lower convective layer
UCL	Upper convective layer
DD	Discovery Deep
KD	Kebrit Deep
KAUST	King Abdallah University for Sciences and Technology
ICP-OES	Inductively Coupled Plasma Optical Emission Spectrometry
VAMPS	Visualization and analysis of the Microbial Structures
OTU	Operational Taxonomic Units
MG-RAST	Metagenomics Rapid Annotation using Subsytems Technology
PeroxiBase	The Peroxidases Database
BacMet	Antibacterial Biocide and Metal Resistance Genes Database
SMTL	SWISS-MODEL Template Library
STRAP	Interactive Structure based Sequences Alignment Program

FET	Fischer's Exact Test
CDD	The Conserved Domain Database
ESBRI	**E**valuating the **S**alt **BRI**dges in Proteins
NQR	NADH Quinone Oxidoreductase
$Fe_{1-X}S$	Pyrrhotite
FeS_2	Pyrite
ZnS	Sphalerite
$CuFeS_2$	Chalcopyrite
(Zn,Fe)S	Marmatite
ECP	Extracellular Polysaccharide
EBP	Extracellular Bacterial Proteins
MGI	Marine Group I
MGII	Marine Group II
SAG	South African Goldmine Group

1. Literature review

1.1. Red Sea brine pools

1.1.1. General description

Red Sea brine pools are challenging and extreme environments, because of anoxic, hyper-saline, high pressure and high temperature conditions. The latter extreme conditions had drawn the attention of scientists in different fields to study these unique environments. To date, about 25 deep-sea brine pools have been discovered in the Red Sea [1-3]. The brine pools were formed over millions of years, as result of tectonic movements of Arabic and African plates. Tectonic movements created fissures in earth crust leading to induction of volcanic activity, expulsion of interstitial brine and resulting in mixing sea water with submarine magma, evaporates, and brine. Consequently, dense hot and metalliferous brine layer were formed in basins, followed by a transition separating layer called brine sea water interface [3-5]. Three interesting anoxic brine pools are the focus of this study: Atlantis II Deep (21°20′ N, 38°5′ E), Discovery Deep (21°17′ N, 38°2′ E) and Kebrit Deep (24°44′N, 36°17′E) (Figure 1). Atlantis II Deep is an irregularly shaped brine pool that is about 2194 m deep and consist of two basins: a main basin of width equal to 13 by 6 km, and a small basin in the north, of width equal to 4 by 3 km [3, 5]. Moreover, Atlantis II Deep shows salinity of 25.7-26.2%, pH about 5.1-5.3, highest temperature (68.2°C) among all Red sea brine pools, and hydrothermal activity, which manifested as observed gradual increase in its temperature over years, from 55.9°C to 68.2°C [5, 6]. Atlantis II brine layer is about 200 m thick, and it is divided into two stratified anoxic layers with substantially different temperatures and salinity: the lower convective layer (LCL) and the upper convective layer (UCL) [5]. Further studies divided the upper convective layer into 3 layers, and It was reported that salinity and temperature increase with depth [2]. The Atlantis II Deep is known to have the richest metalliferous (Fe, Cu, Zn and others) sediments among all Red Sea brine filled basins, together with high dissolved nitrogen, high sulfide, methane and other hydrocarbons content. Also, Atlantis II Deep is likely linked to Discovery Deep via subsurface connections [7-9]. While Discovery Deep brine pool has milder stable

temperature of 44.8 °C, but still has relatively high metals concentration, pH of 6.4, and high salinity (26%). Despite the relative high temperature of Discovery Deep, it did not increase over time as with Atlantis II Deep [5-7].

As for the Kebrit Deep brine pool, it is one of the smallest brine-pools of the Red Sea. The Kebrit pool is a single oval shaped basin of width 2.5 by 1 km, 1549 m deep, and it has a 84 m thick brine layer. It is hypersaline (26%), slightly acidic (pH≈ 5.2-5.5), and has temperature about 23.3°C. The Kebrit Deep is named after the Arabic word for sulfur, out of the strong odor resulting of its high H_2S gas content, also it has high gas content of CO_2 and small amounts of N_2, methane and ethane [2, 5, 6].

1.1.2. Previous microbiological studies

Different microbiological studies, via culture dependent and culture independent (16S rRNA and metagenomic-based) techniques, have been conducted on Red Sea anoxic brine pools. For instance, research work was performed on water column overlying brine pools [10, 11], brine-water interface [6, 12-15], brine pools' sediments [16, 17], and even on brine pools' water [18-20].

In 1969, the first successful isolation of halotolerant *Desulfovibrio* sulfate-reducing bacteria from Atlantis II brine-seawater interface took place [14]. The latter study gave new insights about microbial life in brine pools, after the unsuccessful attempt that gave a false conclusion that Atlantis II harsh conditions made it a sterile environment [21]. Later in 1990, another study reported isolation and characterization of *Flexistipes sinusarabici* anaerobic bacterium, again from Atlantis II brine-seawater interface [13]. While using 16S rRNA primer, five archaeal and six bacterial novel clones have been obtained from Kebrit sediments in a more recent study [16], which was followed by a study, by the same researcher, about microbial communities in Kebrit brine-seawater interface [12]. With development of advanced high-throughput DNA sequencing technologies, new series of studies revealed more secrets about microbial communities and their metabolic activities in brine pools. For instance, a 16S rRNA survey on bacterial and archaeal communities

inhabiting the water column overlying both Atlantis II and Discovery brine pools concluded that generally the water column overlying different brine pools has the same microbial communities composition [10]. Another recent metagenomic study compared between the metagenome of the water column overlying Atlantis II deep and others from different marine environments from all over the world, in order to investigate changes in microbial genomes in response to different conditions of oxygen and light [11]. An interesting recent research also highlighted the relation between sediment geochemistry and microbial communities inhabiting sediments from Atlantis II deep, Discovery deep, a brine influenced site and Chain Deep [17].

As for brine water, a recent metagenomic study identified dominant bacterial communities and compared enrichment of aromatic degradation pathways in both metagenomes of lower convective layers of Atlantis II and Discovery brine pools [19]. Using the same samples of the latter study, another more comprehensive comparative analysis functionally compared the same data with reference metagenomes [20]. Eventually, a phylogenetic study discussed microbial communities in brine water and the overlying water column of both Atlantis II and discovery Deep via 16S rRNA pyrosequencing [18].

Yet none of the above mentioned studies functionally investigated metagenomes of brine water from Kebrit Deep or Atlantis II upper convective layer. In addition, no 16S rRNA survey has been conducted before on Kebrit Deep brine water. To the best of our knowledge, this study is the first to investigate and compare microbial metal interaction in Atlantis II, Discovery and Kebrit Deep brine water. Likewise, it is the first research work to study Kebrit Deep brine water using both: 16S rRNA pyrotags and shot-gun 454-pyrosequencing.

1.2. Essential and non-essential metals

Metals are classified to be either essential or non-essential metals according to their biological roles. Essential metals have indispensable biological functions that no other organic compounds can fulfil, while non-essential metals are biologically unimportant and potentially lethal. Nevertheless, the excessive abundance of even essential metals has toxic

effects to microbial cells. Essential metals as: iron (Fe), copper (Cu), zinc (Zn), manganese (Mn), cobalt (Co), nickel (Ni), sodium (Na), magnesium (Mg), potassium (K), calcium (Ca), vanadium (V), chromium (Cr), selenium (Se), and molybdenum (Mo) are structural components of proteins, DNA, cell membranes and act as cofactors in variety of biochemical reactions. Interestingly, about 50% of known proteins rely on metals to function, especially in catalysis and electron transfer**.** In contrast, non-essential metals as mercury (Hg), arsenic (As) silver (Ag), gold (Au), lead (Pb), aluminum (Al), tellurium (Te) and cadmium (Cd) can show high toxicity to microbial cells at very low concentration [22-24]. Because of the antimicrobial effect of some metals, they have been used in many applications as bactericidal coating for devices and different tools. Interestingly, some metals proved to even disrupt antibiotic-resistant biofilms[25]. Generally bactericidal metals, exert their toxicity through chemical and physical interaction with cellular donor ligands [23, 24].

1.3. Metal chemistry

Oxygen, nitrogen and sulfur in protein structure bind selectively to metals. The selectivity in binding metals with the latter atoms is mainly related to atomic structure of metals and coordination geometry, which guarantee that the correct metal will bind to the protein in order to function and fold properly. Nonetheless, when metal homeostasis is disrupted, other incorrect metal could bind. Additionally, mimicry in structure between metal ions and other cofactors may hinder correct binding and cause proteins dysfunction [23, 26, 27].

According to Pearson's acid base theory, metals are classified into hard acids (Fe^{3+}, Co^{3+}, Ga^{3+}, Cr^{3+},Al^{3+}, $Ca^{2+,}Mg^{2+}$,Na^{+},K^{+}), soft acids (Cd^{2+}, Hg^{2+},Hg^{+},Cu^{+},Au^{+},Ag^{+}) and borderline acids (Fe^{2+},Cu^{2+},Co^{2+},Zn^{2+},Pb^{2+}, Ni^{2+},Bi^{3+}). Hard acids often have small ionic radius, high electronegativity and high oxidation state, while soft acids have large ionic radius, low electronegativity and low oxidation state. Borderline acids and soft acids usually binds strongly with soft bases as protein sulfhydryl and thiol groups, while hard acids react

with hard bases as phosphate, amine, sulfate, carbonate, carboxylates, and nitrate groups [28, 29].

Moreover, regarding redox potential (measure of tendency to gain electrons and become reduced), metals are classified to redox active and redox inactive metals. Unlike redox inactive metals, redox active metals have more than one oxidation state, as their outermost atomic orbital can bear different number of electrons. Interestingly, possibility of accommodating different numbers of electrons, enable redox active metals to take part in transfer of electron in most important biochemical processes as respiration and photosynthesis. Different studies showed that redox potential of metals and their toxic interaction with biomolecules are correlated. Also other conditions affects metals chemical species and oxidation state: like surrounding temperature, presence of oxygen, metals' ionic strength and pH. For instance, in aerobic conditions, oxidation of Fe^{2+} favorably takes place to Fe^{3+}[23, 24, 30, 31].

1.4. Mechanisms of metal resistance

According to chemical and physical properties of metals, microorganisms differently resist and adapt to their toxicity. Yet, there are main resistance strategies that summarize all resistance mechanisms that most bacteria and archaea generally follow (Figure 2).

1.4.1. Control of metals' transport

Bacteria and archaea can control the transport of metals in and out of their cells. Through regulation and expression of membrane metal transporters, bacteria can decrease certain metal uptake or increase its efflux [22, 32, 33].

1.4.2. Sequestration

Another mechanism used by microorganisms is sequestration or precipitation of toxic metals. Some bacteria have the ability to use siderophores (iron chelating compounds) and extracellular polymers, cell-associated polysaccharides, and surface proteins to chelate certain metals, as a defense in case of high concentration of metals in surrounding media. As a result of metal chelation, metals may be precipitated or present as a complex that can be more effluxed or less uptaken. Interestingly, some bacteria can precipitate and trap metals in their periplasmic space or cytoplasm, in form of crystals, oxides, sulfides, and can bind metals to proteins forming aggregates [22-24, 34].

1.4.3. Metabolic by-pass

Microorganisms can direct metabolites towards alternative pathways, if the original metabolic pathways had metal disrupted proteins. In some cases, bacteria can synthesize modified proteins lacking metal binding sites [23, 35].

1.4.4. Redox modification

Some microbial enzymes have the ability to change oxidation state of metals by either oxidation or reduction. Changing metals oxidation state affect metal toxicity, where some metals become less toxic and less reactive. Also oxidation or reduction of metals may cause metal precipitation or formation of organic-metal compounds [24, 36, 37].

1.4.5. Repair

Different oxidoreductases, antioxidants and cellular chaperons are recruited by microbial cells to repair different cellular molecules that undergone oxidation by metals or metal derived reactive oxygen species (ROS) [23, 24, 38].

1.5. Mechanisms of metal toxicity

Metals induce toxicity by various mechanisms according to their chemistry. Most probably bacteriostatic and bactericidal effects of metals arise from synergistic effect of different mechanisms.

1.5.1. Metal catalyzed ROS production and antioxidant depletion

An increase in intracellular ROS production in bacteria and upregulation of genes involved in ROS scavenging, was reported upon exposure to toxic doses of certain metal ions such as Cu^{2+}, Fe^{2+},Te^{4+}, As^{3+} and Cr^{6+} [23, 39-42]. Interestingly, *E. coli* DNA damage was caused by just regulation defects in Fe metabolism [39]. Hence, it was concluded that cellular damage is in part caused by metal catalyzed oxidation reactions [23, 39-42]. In brief, three main mechanisms were suggested to explain increased ROS generation in case of high metal exposure.

First, aerobic respiration generates hydrogen peroxide (H_2O_2) and superoxide anion (O_2•−) as byproducts. The latter byproducts may initiate metal-catalyzed free radical chain reactions or undergo oxygen transfer by redox active metals in a chemical reaction called Fenton reaction. In Fenton reaction, hydrogen peroxide undergoes iron-catalyzed decomposition yielding hydroxide ion (OH^-) and the extremely reactive hydroxyl radical ($OH^{\bullet}$) (equation 1), which is capable to oxidize various organic compounds. Consequently, Fenton reagent (H_2O_2 + iron salts) is used to detoxify polluted water by oxidizing organic pollutants [43]. *In vitro* experiments showed that oxidized iron (Fe^{3+}) can be reduced by superoxide anion ($O_2^{\bullet-}$) to produce Ferrous ions (Fe^{+2}) and oxygen (equation 2). Haber and Weiss described the net reaction of hydroxyl radicals' production, when superoxide reacts with hydrogen peroxide in the presence of iron (equation 3). *In vivo*, there are multiple reducing agents as glutathione (GSH), ascorbic acid, NADPH and NADH, that can reduce Fe^{3+} in cells [24, 30, 44]. Beside iron, other transition metals can catalyze Fenton reaction *in vitro* e.g. Co, Cu, Cr, Ni, and V. While *in vivo*, it is hard to predict which metals can catalyze Fenton reaction, as it depends on many other factors, such as relative reduction

potential, pH, and coordinating ligands [24, 30, 45]. Unlike other transition metals, some studies show that manganese can participate in protecting cells from ROS [46, 47].

$$Fe^{2+} + H_2O_2 \rightarrow Fe^{3+} + OH^{\bullet} + OH^{-} \quad (1)$$
$$Fe^{3+} + O_2^{\bullet-} \leftrightarrow Fe^{2+} + O_2 \quad (2)$$
$$O_2^{\bullet-} + H_2O_2 \leftrightarrow O_2 + {}^{\bullet}OH + OH^{-} \quad (3)$$

Second, some transition metals can interact with cellular donor ligands, as iron sulfur [4Fe–4S] clusters [48, 49]. The latter destructive interaction can release more Fenton-active iron in cells, increasing ROS. That's why some studies reported increased microbial intracellular ROS even if the interacting transition metals are Fenton-inactive like Ga, Hg, and Ag [23].

Third, many *in vitro* studies showed that ROS generation can be increased by production of intermediate sulfur radicals that are formed via reduction of metals such as Te^{4+},Fe^{3+}, As^{3+}, Cr^{6+}, and Cu^{2+}, by thiol groups. Also in some cases the latter reduction reaction can produce Fenton-active metals as proved in case of Cr^{6+} that upon reduction becomes Cr^{5+},Cr^{4+}, and Cr^{3+}, but up till now it is not confirmed to take place *in vivo* [24, 38].

Eventually, metal oxyanions, soft acids (Cd^{2+}, Hg^{2+},Hg^{+},Cu^{+},Au^{+},Ag^{+}) and borderline acids (Fe^{2+},Cu^{2+},Co^{2+},Zn^{2+},Pb^{2+}, Ni^{2+},Bi^{3+}) favorably bind to intracellular thiols by formation of covalent bond with sulfur. The latter reaction result in depletion of thiol compounds such as glutathione that act directly as ROS scavenger and participate in repair of oxidized protein thiols by cellular thiol–disulphide exchange enzymes. Hence, depletion of such antioxidants renders cells unprotected against destructive oxidizing agents or even other metal species [38, 50, 51].

1.5.2. Metal interaction with proteins

Side chains of few amino acid residues in some proteins may undergo specific metal ion-catalyzed oxidation yielding carbonyl derivatives, which has been particularly confirmed in case of threonine, proline, lysine, arginine, and histidine. Some studies on *E.coli* pointed out that amino acid residues lying at glutamine synthetase metal binding sites are especially vulnerable to metal catalyzed oxidation, which generally can lead to loss of enzyme activity or even its degradation [52, 53].

Some metalloenzymes as *E.coli* threonine dehydrogenase and peptide deformylase have Fe in their structure and they coordinate Fe^{2+} using cysteine residues that are vulnerable to oxidation via Fenton reaction. Upon oxidation, cysteine is modified yielding sulphonic or sulphinic forms [54].

In some enzymes, iron-sulfur [4Fe–4S] clusters are crucial for catalytic activity. Previous research showed that iron-sulfur clusters can be destroyed either in presence of oxygen via ROS, or even in anoxic conditions by metals [48, 49]. In one study, toxic doses of hydrogen peroxide (H_2O_2) and superoxide anion ($O_2\bullet-$) lead to inactivation of isopropylmalate isomerase dihydroxy-acid dehydratase enzymes, by destruction of iron-sulfur clusters [44]. Likewise, under anoxic conditions Cu^{1+} was found to modify iron-sulfur clusters in some enzymes to [3Fe–4S] form, which lead to enzyme deactivation *in vivo* [48]. Unlike Cu^{1+}, Te^{4+} can only destroy enzymes' iron-sulfur clusters in aerobic conditions[55].

Ionic mimicry is also another cause of protein loss of activity, where certain metals within proteins may be substituted with another incorrect metal that mimic the original one in ionic structure. For instance, it was confirmed that the activity of δ‑aminolevulinic acid dehydratase enzyme was inhibited when Zn^{2+} was displaced with Pb^{2+} from its active site [23, 56].

Another study showed that even if the metal displacement did happen in a site other than the active one, metal substitution might still lead to inhibition of enzyme activity. For

instance, *E. coli* fructose‑1,6‑bisphosphate aldolase lost its activity when Zn^{2+} at non catalytic site was displaced with Ni^{2+} [23, 57].

1.5.3. Metal interaction with bacterial membranes

Metal ions may become adsorbed to polymers of highly electronegative groups in bacterial membranes. Accordingly, it was hypothesized that metal toxicity may be induced through acting on sites of bacterial membranes [58].

Furthermore, some metals such as Ag inactivate NADH quinone oxidoreductase (NQR) of electron transport chain in bacteria and may cause proton leakage as a mechanism for toxicity [59, 60]. It was also reported that metal toxicity may be induced via lipid peroxidation in bacteria, as in case of Cu^{2+}. The latter mechanism of toxicity may explain the bactericidal effect of Cu surfaces [61].

1.5.4. Metal induced starvation

Some metals may interfere with nutrient assimilation in bacteria causing starvation and death. For instance, Ga^{3+} deregulate gene expression of PvdS Fe-responsive transcriptional regulator, leading to uptake inhibition of Fe^{3+} needed for bacterial growth in *P. aeruginosa* [62].

1.5.5. Metal induced DNA damage

Fe-mediated Fenton reaction has been suggested to cause DNA damage in *E. coli.* Studies have shown that disruption in Fe homeostasis, and Fe increase in cells have a genotoxic effect on bacterial cells [40, 63]. One study confirmed that Fe chelators save *E.coli* cells from DNA damage when exposed to H_2O_2, which has not been proved in case of other metals [64]. Moreover, some metals in their toxic concentration proved to be mutagenic in bacteria, as in case of Sb^{3+},Mo^{4+},As^{3+},Cr^{6+},Co^{2+},Cd^{2+}, Mn^{2+}, and some organic

mercury compounds. While other metals do not have mutagenic effect on bacteria even in toxic concentration, as in case of Al^{3+},Ag^{+},Pb^{2+},Te^{4+},Cu^{2+} and Ni^{2+} [23, 65, 66].

1.6. Metagenomic revolution

Classic culture dependent techniques have failed to give accurate estimation of microbial communities harboring different environments. Recently, the metagenomic revolution has changed microbiologists' view of studying microorganisms and solved many of microbial culturing problems. In fact, culture media couldn't mimic some natural environments with special conditions as presence/absence of nutrients, surfaces, inhibitory compounds, necessary symbionts, media gas composition, pressure, metals, salts, temperature, and toxic wastes. Consequently, only 0.1% of the microbes could be cultured [67, 68].

In 1998, the term "metagenomics" was first introduced by Handelsman and her colleagues and was defined as a cultivation-independent technique where all DNA is extracted collectively from a certain niche, which is commonly followed by DNA cloning or/and sequencing [67, 69]. Recent emergence and advancement of high throughput sequencing techniques (Roche/454 GS FLX Titanium sequencer, Illumina Genome Analyzer, Applied Biosystems SOLiD, etc.) has drastically altered metagenomics field, and made it feasible to rapidly generate enormous amounts of metagenomic sequences at relatively low cost [70, 71]. Through DNA sequencing and assembly of large genomic data, investigation of different metabolic pathways and genes within genomes of microbial communities living in certain environments, was made possible [68, 72]. Moreover, identification of microbial communities in a certain niche became easier by using protein-encoding or 16S rRNA-encoding DNA sequences. Interestingly, the use of the metagenomics approach has led to isolation of different novel thermostable and halotolerant proteins from extreme environments, which have many applications [73, 74]. For isolation of novel proteins, two main approaches are followed: function-based or sequence-based techniques. Function based technique depends on cloning genes of interest, and screening for expressed gene product using specific substrates, while sequence based technique rely

on comparing metareads to sequences within protein databases to assess its function and novelty [67, 68].

Using metagenomic approach, we aim to compare between free living metal-resistant prokaryotic communities in different harsh brine water environments (ATII, DD, and KD), identify main mechanisms of microbial metal interaction/ metal resistance in different brine water layers, and correlate results with specific high metal/s concentration in selected brine water. Accordingly, we would learn how prokaryotic communities resist and induce changes to the surrounding environment, and how geochemical conditions shaped abundance of microbial communities and affected their microbiomes.

2. Materials and Methods

2.1. Samples collection, DNA extraction and pyrosequencing

Water samples were collected during KAUST Red Sea *R/V Aegaeo* expeditions in Spring of 2010 and 2011, from three brine pools: Atlantis II Deep (LCL and UCL) (21° 20′ N, 38° 5′ E), Discovery Deep (21° 17′ N, 38° 2′ E) and Kebrit deep (24°44′N, 36°17′E). Water samples were collected by 10 Niskin bottles attached to rosette. About 120 litres from each brine layer was sequentially filtered by different pore sized filters (3 μm, 0.8 μm and 0.1 μm). Used filters were mixed-nitrocellulose/cellulose acetate ones (Millipore, Ireland) . Sucrose buffer was then used to protect DNA until extraction. As described by Rusch et al, DNA was extracted from the microbial cells trapped on the 0.1μm filters [75]. DNA quantification was done using the Quant-iT™ PicoGreen® dsDNA kit (Invitrogen, USA), and Nano Drop 3300 Fluorospectrometer (Thermo Scientific, USA). Four libraries were constructed for the metagenomes as described by GS FLX Titanium library guide (Roche, Germany). Universal V6-V4 primers for bacteria and archaea were utilized for PCR amplification of 16S rRNA genes. Finally, both 16S rRNA amplicons and the four metagenomes were pyrosequenced by 454 GS FLX Titanium technology (454 Life Sciences).

2.2. Chemical profiling

Water samples from the three brine pools ATII-LCL, DD, and KD were analyzed for various metals and a range of non-metals, using Varian Vista MPX ICP-OES system (MEDAC LTD, UK) . Units of elements' concentrations were all unified to be in ppm.

2.3. Computational analysis

Taxonomic assignment of 16S rRNA reads and operational taxonomic units (OTUs) to major bacterial and archaeal taxa was done via website of the Visualization and Analysis of Microbial Population Structures (VAMPS) [76]. UCLUST tool on VAMPS website, was used to cluster 16S rRNA sequences into OTUs with identity threshold ≥ 97% [76]. Two clustering processes were used: one for bacterial 16S rRNA datasets generated by bacterial V6-V4 primers and the other was for archaeal 16S rRNA datasets generated by archaeal V6-V4 primers. To eliminate 16S rRNA pyrotags shared between brine water and the overlying water column, brine water datasets were clustered together with ATII overlying water column 16S rRNA datasets previously obtained from different depths: 50m, 200m, 700m, 1500m [11].

After subtracting common pyrotags from brine water OTU clusters, OTUs showing un-significant difference in abundance between brine pools were eliminated using two-tailed Fisher's exact test [77] via R software (< 0.05, Bonferroni-corrected) [78]. Moreover, Fisher's exact test was used for statistical filtering of all metagenomic reads in all functional analyses within this study .

The ATII-LCL, ATII-UCL, DD, KD 454-metagenomes were deposited in MG-RAST server (**M**eta**g**enomics **R**apid **A**nnotation using **S**ubsytems **T**echnology) [79, 80]. Using MG-RAST, metagenomes were subjected to hierarchical annotation within SEED subsystems database (E-value cutoff = $1e^{-5}$, minimum % identity cutoff =60%) [80]. Through SEED functional classification of metagenomic reads, examination of metal resistance, iron transport/metabolism and membrane transport of metals was performed. As a confirmatory experiment, a BLASTx search against BacMet database of 444 experimentally confirmed metal-resistance genes (University of Gothenburg, Sweden) [81], which had average sequence length of about 343 amino acids (E-value cutoff = $1e^{-5}$, minimum % fraction conserved cutoff = 60%). Additionally, metagenomes were subjected to a BLASTx search against PeroxiBase (the peroxidases database, http://peroxibase.toulouse.inra.fr/**)** [82], but only PeroxiBase bacterial and archaeal

sequences were used (1,497 sequences). PeroxiBase enzyme sequences were of average length of 427 amino acids (E-value cutoff = $1e^{-5}$, minimum % fraction conserved cutoff =60%).

ATII-LCL metagenome assembled contigs were searched by BLASTx against 3,718 sequences of arsenate reductase enzyme (BRENDA, The Comprehensive Enzyme Information System, www.brenda-enzymes.org) [83]. Metagenomic genes showing more than 90% coverage and maximum E-value= $1e^{-5}$, were subjected to BLASTx search against NR (Non-redundant) protein database and Conserved Domain Database (CDD) [84]. Two ORFs from the same contig were coding for large and small subunits of arsenite oxidase (ArOX), and having essential catalytic domains, were further investigated . Three-dimentional models were generated for these two ORFS by homology modeling against crystal structure of ArOX from *Alcaligensis faecalis* (SMTL id: 1g8k.1), using SWISS-MODEL (http://swissmodel.expasy.org) [85]. Templates used for building 3D models showed 69.68 % sequence identity with ATII-LCL large subunit, and 60.9 % sequence identity with ATII-LCL small subunit. The same templates (*A. faecalis*) were used to build 3D models for *Cupriavidus basilensis* ArOX subunits, showing 69.96 % sequence identity with *C. basilensis* large subunit, and 59.4 % sequence identity with *C. basilensis* small subunit. Additionally , The ATII-LCL and *C. basilensis* ArOX subunits were examined for amino acids composition by ProtParam tool (http://web.expasy.org/protparam/). Finally, sequence alignment between ATII-LCL ArOX and *C. basilensis* ArOX subunits was done by STRAP (Interactive **Str**ucture based Sequences **A**lignment **P**rogram, http://www.bioinformatics.org/strap/aa/) [86].

3. Results

3.1. 16S rRNA pyrotag datasets

Four brine water layers: Atlantis II lower convective layer (ATII-LCL), Atlantis II upper convective layer (ATII-UCL), Discovery Deep (DD), and Kebrit Deep (KD), generated 136,569 pyrotag reads (Table 1). Of 136,569 pyrotag reads, 66,184 pyrotag reads were assigned to bacteria, 69,149 pyrotag reads represented archaea, and 1,236 were unassigned reads. ATII-UCL generated the highest number of bacterial (21,506) and archaeal (25,956) reads, while ATII-LCL showed the lowest number of bacterial reads (11,546). However, DD generated the lowest number of archaeal reads (11,838) and the highest number of unassigned pyrotag reads (775). Brine pools' water 16S rRNA pyrotag reads generated from the Atlantis II overlying water column together with the four brine water layers, were clustered into operational taxonomic units (OTUs) (as described in Materials and Methods). The total utilized OTUs were 189 OTUs, after exclusion of both: 16S rRNA sequences shared between brine water and the overlying water column, and statistically un-significantly abundant OTUs (Fisher's exact test-as described in materials and methods). Of 189 OTUs, 98 OTUs were assigned to archaea, 88 OTUs represented bacteria, and three OTUs were unassigned.

3.2. Dataset of shotgun pyrosequencing metagenomic libraries

454-shotgun-pyrosequencing were carried out for the same aforementioned samples. Sequencing of DNA retrieved from 0.1 μm filters of the four brine water layers generated 3,612,992 metagenomic reads. Statistical data of the four metagenomes, computed by MG-RAST, are summarized in Table 2. This also allowed us to extrapolate the number of sequences containing ribosomal RNA genes, the number of predicted protein coding sequences with known or unknown functions, and number of sequences that do not contain rRNA genes or predicted proteins (Table 2).

3.3. Taxonomic assignment of OTUs to major bacterial groups

Bacterial communities in the four brine water layers showed great richness (Figure 3). Only statistically significantly abundant OTUs of ≥1% relative abundance are presented in this study (Fisher's exact test). To eliminate potential contamination from the overlying water layer, we excluded 16S rRNA sequences common between brine water and the overlying water column clusters (described in Materials and Methods).

Proteobacteria dominated all brine water layers except those in ATII-LCL, where Firmicutes (64.22%), represented by *Paenibacillus* genus dominated. Proteobacteria were detected in ATII-LCL, but with relatively lower abundance (23.6%), and were represented by the following genera: *Alteromonas* (15.68%), *Cupriavidus* (2.47%), unassigned genus of family *Enterobacteriaceae* (2.09%), *Brevundimonas* (1.22%), *Pseudomonas* (1.1%) and *Halomonas* (1.04%). Despite the fact that Proteobacteria were detected in all brine water layers, this phylum was represented by 20 different genera in different brine layers, each of which had its own exclusive genera except for the four genera: *Altermonas, Halomonas, Cupriavidus,* and *Acinetobacter* that were shared between brine water layers. Generally, the latter four genera were the only shared bacterial genera between brine water layers (Supplementary Table 1).

Proteobacteria were highly abundant (83.64%) in ATII-UCL, and were represented by 3 genera: *Phyllobacterium* accounted for (53.96%) of total reads, then *Cupriavidus* genera (16.31%), and *Enhydrobacter* (13.37%). While the lowest number of reads was for *Deferribacteres* represented by *SAR406* (10.21%).

Similarly, Proteobacteria dominated the bacterial community in DD, and were represented by seven genera: *Halomonas* (43.49%), *Alteromonas* (6.79%), *Loktanella,* (4.31%), *Sulfitobacter* (3.14%), *Erythrobacter* (3.09%), *Acinetobacter* (2.37%), and *Psychrobacter* (1.01%). Furthermore, *Actinobacteria* were detected in DD (1.94%) represented by unassigned family of order *Actinomycetales* (Supplementary Table 1).

We detected 10 genera of Proteobacteria in KD. This included unclassified *Deltaproteobacteria* (1.98%), and unclassified genus of family *Comamonadaceae* (1.07%). The abundant genera included: *Acidovorax* (44.07%), *Roseateles* (26.62%), *Cupriavidus* (2.66%), *Pseudoalteromonas* (2.64%), *Dechloromonas* (2.13%), *Desulfovermiculus* (1.98%), *Aquabacterium* (1.83%) *Acinetobacter* (1.68%), *Sphingomonas* (1.44%) and *Delftia* (1.29%). Other unclassified phyla were detected in KD, as OP1 (3.78%).

3.4. Taxonomic assignment of OTUs to major archaeal groups

In ATII-LCL, ATII-UCL, and DD archaeal communities were comprised of Euryarchaeota and Crenarchaeota (Figure 3, Supplementary Table 2). In ATII-LCL, *Euryarchaeota* dominated and were represented by unassigned genus of family Marine Group II (24.84%), unassigned family of order Marine Benthic Group E (4.47%), and family *Methanosaetaceae* of genus *Methanosaeta* (3.9%), while Crenarchaeota were represented solely by class Marine Group I (14.46%). In contrast, Crenarchaeota dominated the archaeal community in ATII-UCL, showing 87.31% relative abundance, beside the presence of relatively less abundant Euryarchaeota in form of unassigned family of order Marine Benthic Group E (4.71%), family *Methanosaetaceae* of genus *Methanosaeta* (2.81%),and unassigned genus of family Deep Sea Hydrothermal Vent Group 6 (1.11%).

While uncultured *Thermoplasmata* of the South African Goldmine (SAG) Group dominated in both KD and DD by 96.53%, and 50.82% relative abundance, respectively, where Euryarchaeota monopolized all archaeal pyrotags in KD. Unlike KD, other members of Euryarchaeota were detected in DD: unclassified ST-12K10A lineage (SA1 group) with relative abundance (27.09%), and members of order *Halobacteriales*, which were represented by unassigned genus of family *Halobacteriaceae* (11.87%), genus *Halomicrobium* of family *Halobacteriaceae* (2.43%), and unassigned genus of family MSP41 (1.61%). Finally, Crenarchaeota was barely detected in DD and represented by unassigned order of class Terrestrial Hot Spring Group (1.04%).

3.5. Chemical profiling of water from brine pools

Out of the four water samples, we analyzed the chemical composition (21 different elements and metals) of three water samples: one from each brine pool (Table 3). ATII-LCL had the highest concentration of iron (47.6 ppm), manganese (78.9 ppm), gold (1.9 ppm), platinum (0.5 ppm), barium (1.9 ppm), and zinc (3.9 ppm). Copper and lead contents were relatively low (0.1 ppm each), and were only detected in ATII-LCL. Similarly, ruthenium and tin were only detected in relatively low concentrations in KD (0.1 ppm each). In KD, boron, phosphorous, and silicon showed the highest abundance of 20.8 ppm, 0.7 ppm, and 5.4 ppm, respectively. While arsenic, aluminum, tungsten, strontium showed comparable abundance in different sites. Cations as potassium, calcium, magnesium, and sodium were present in high amounts in all samples, especially sodium. ATII-LCL had the highest content of potassium (2700 ppm) and calcium (5300 ppm), while KD showed the highest relative concentration of magnesium (2500 ppm) and sodium (94100 ppm).

3.6. Screening the samples for peroxidases using PeroxiBase (the peroxidases database)

To understand more about the impact of high metal abundance on the chemistry of the anoxic brine water layers, we invistigated the four metagenomes were investigated for the presence of peroxidases enzymes using the PeroxiBase database [82] (bacterial and archaeal sequences only). Fisher's exact test (FET) [77] was used to filter insignificant peroxidases reads. ATII-LCL showed the highest relative abundance of peroxidases among all our Red Sea metagenomes (Table 4). The number of reads and relative abundance for ATII-LCL, ATII-UCL, DD, and KD metagenomes were 914 (0.08%), 319 (0.048%), 161(0.024%), and 53 (0.005%), respectively. Diverse haem and non-haem peroxidases were detected in metagenomes. In ATII-LCL and ATII-UCL, the highest relative abundance was for the haem catalase (LCL: 250 reads, UCL: 97 reads) followed by the non-haem glutathione peroxidase (LCL: 203 reads, UCL: 70 reads). In DD, the highest relative abundance was for non-haem atypical 2-Cysteine peroxiredoxin, which showed only (47

reads). While in KD, non-haem carboxymuconolactone decarboxylase was the most abundant (21 reads).

3.7. Relative abundance of metal resistance genes and metal transporters, using SEED Subsystems database

Using MG-RAST analysis server , we annotated the four metagenomes within SEED subsytems database [80]. The main focus was to examine the abundance and enrichment of the sets of genes related to microbial metal interaction and resistance, to assess the effect of the metal rich environment of the brine water layer on bacterial and archaeal communities. Additionally, this will shed light on the different mechanisms used by the extremophile communities to avoid metal induced toxicity. We assessed the abundance of genes coding for cobalt-zinc-cadmium, copper, mercury, chromate and arsenic resistance. After statistical filtering of metal resistance reads (using FET) [77], we determined the relative abundance of metal resistance genes. They comprised for ATII-LCL, ATII-UCL, DD and KD: 14,353 (1.25%), 4,671 (0.7%), 1,121(0.16%), and 572(0.05%), respectively (Table 5 - Supplementary Table 3). Cobalt-zinc-cadmium resistance genes were the most abundant in all our Red Sea brine metagenomes except KD, where copper resistance genes (335 reads - 0.029%) were the most abundant. Both ATII-LCL and UCL had the same pattern of increase in relative abundance of metal resistance genes, starting from the most abundant cobalt-zinc-cadmium, followed by copper, mercuric, chromate and ending with the least abundant arsenic resistance genes. Disregarding chromate resistance genes, which had almost zero relative abundance in both DD and KD, DD followed the same pattern of increase in relative abundance of metal resistance genes as ATII-LCL and UCL, while KD showed a unique pattern of increase in relative abundance, showing copper as the most abundant (0.029%), followed by cobalt-zinc-cadmium (0.014%), arsenic (0.006%), mercury (0.001%), and chromate resistance genes (0%). Our analysis also presents a variety of genes involved in metal resistance as detoxifying enzymes, efflux pumps, resistance proteins and others (Supplementary Table 3). The highest relative abundance for ATII-LCL was for the cobalt-zinc-cadmium resistance proteins in (2821 reads), followed by ATII-LCL cobalt-zinc-cadmium resistance protein CzcA (2375 reads), ATII-LCL copper-translocating P-type

ATPase (2074 reads), and ATII-LCL multicopper oxidases (1049 reads). To confirm abundance of metal resistance genes in our metagenomes, metal resistance was examined again within BacMet database of **experimentally confirmed** resistance genes. Results confirm the data generated utilizing the SEED Subsystems database (Supplementary Table 4).

3.8. Relative high abundance of genes involved in iron transport and metabolism in the Atlantis II-LCL

As iron was specifically abundant in ATII site (47.6 ppm), and it is involved in different metabolic activities, the impact of high metal abundance in this samples was assessed. We examined the enrichment of iron metabolism and transport genes utilizing the SEED Subsystems database. The highest abundance of such genes were observed in ATII-LCL (2259 reads-0.198%), ATII-UCL (673 reads- 0.102%), followed by DD (306 reads-0.046%) and KD (195 reads- 0.017%) as shown in Table 6 (Supplementary Table 5). Highest relative abundance of ferrichrome-iron receptor genes (322 reads), ferric iron ABC transporter- iron binding protein (171reads), ATII-LCL ferric iron ABC transporter – permease protein (170 reads), and finally putative high-affinity iron permease genes (165 reads) were observed in ATII_LCL. These results results correlated with the measured iron concentration in the samples.

3.9. Examination of membrane transport genes of manganese, zinc, molybdenum, nickel and cobalt transport

Beside iron, the profusion of other biologically essential metals in these environments, affects their transport across microbial biological membranes. Accordingly, enrichment of genes involved in metal membrane transport, were investigated. Relative abundance of genes encoding for membrane metal transport of manganese, zinc, molybdenum, nickel and cobalt within SEED Subsystems database were investigated. As with iron the reads/percentage was highest in ATII-LCL followed by ATII-UCL, DD and KD (1,641/0.144%), (511/0.077%), (119/0.018%), and (67/0.006%) respectively (Table 7 -

Supplementary Table 6). Manganese transporters were most represented in ATII-LCL (914 reads) and ATII-UCL (321 reads), and their read numbers made up more than half of the total reads detected in the later metagenomes. Following manganese transporters, zinc transporters were represented by (473 reads) in ATII-LCL and (100 reads) in ATII-UCL, while molybdenum transporters reads were: (204 reads) for ATII-LCL, and (75 reads) for ATII-UCL. Nickel and cobalt transporters were the least abundant by (50 reads) for ATII-LCL and (15 reads) for ATII-UCL. In DD, zinc transporters (62 reads) were more abundant than copper ones (29 reads), followed by molybdenum transporters (25 reads), while nickel and cobalt transporters were the least abundant (three reads). All metal membrane transporters in KD, were very few and almost absent.

Figure 4. shows a graph comparing between ATII-LCL, ATII-UCL, DD, and KD brine water samples, in terms of relative abundance of genes involved in: mental resistance, iron metabolism/transport, membrane metal transport, and encoding peroxidases

3.10. *In silico* identification of metagenomic arsenite oxidase enzyme

Arsenite oxidase (ArOX) is an example of enzymes used by microbial communities in metal detoxification. Assembled contigs from metagenomes were mined for a unique arsenite oxidase enzyme. Arsenite oxidase is a heterodimeric enzyme containing a large and a small subunit. Two ORFs for arsenite oxidase were identified on an ATII-LCL contig: both ORFs (828 and 172 amino acid residues) showed the highest identity to arsenite oxidase large and small subunit of *Cupriavidus basilensis.*

Using the Conserved Domain Database (CDD), we confirmed that both ArOX large catalytic subunits harbor the molybdopterin cofactor and the [3Fe-4S] cluster binding sites (Accession: cd02756) with E-value=zero for both (Figure 5). As for both ArOX small subunits, also presence of Rieske-type [2Fe-2S] cluster, and subunit interaction site, was confirmed (Accession: cd03476), where E-value: for ATII-LCL ArOX = 1.39e-42 , and that of *C. basilensis* = 1.91e-67 (Figure 6).

Table 8 shows amino acids composition of ATII-LCL and *Cupriavidus basilensis* arsenite oxidase subunits based on: Expasy protparam tool, 3D models generated by Expasy swiss-model tool, salt bridges prediction by ESBRI tool.

4. Discussion

Our data showed to be rich in information about free living microbial communities harboring brine water, metal abundance, and evolution of microbial microbiomes to tolerate and adapt to metal toxicity. Analyses of our datasets together with reviewing literature enabled us to describe different patterns of microbial metal interaction, which might be taking place in brine pools.

4.1. Atlantis II Deep (ATII)

Our chemical analysis together with previous studies confirm huge metal content in ATII-LCL brine water and sediments. ATII metalliferous sediments are known to have the highest metal content among all brine filled deeps (≈ 90 million tons) [1, 87]. Massive sulfide minerals have been identified in ATII as pyrrhotite ($Fe_{1-X}S$), pyrite (FeS_2), sphalerite (ZnS), chalcopyrite ($CuFeS_2$), marmatite ((Zn,Fe)S), amorphous sulfides of (Fe/C/Zn), and Cu-sulfosalt sulfide minerals [1]. The approximate value of ATII sulfide mineral deposits have been estimated to be 3.11-8.21 billion$ [88]. Regarding metal concentrations in brine water, our results showed that ATII-LCL was unique in its high iron (47.6 ppm) and manganese (78.9 ppm) content, which agrees with most recent studies that show a significant increase in ATII-LCL iron and manganese relative to DD and KD [6, 18]. Though geochemical measurements, including ours, are not exactly equal in various studies, yet they mostly follow the same pattern. Discrepancies between metal measurements in different studies principally arise from using different sampling, handling and analysis techniques, in addition to the fact that dissolved metal concentrations are not uniformly distributed in the same brine layers. For example, in ATII-LCL, concentrations of iron, manganese and zinc are highest at the central part of the southwest basin. However, concentrations of the same metals are lowest at the north basin [1].

Several factors may have contributed to high metal concentration in AII-LCL brine water. First, water just overlying sea bed sediments creates a mobile medium for the runoff,

leach, circulation and transfer of metals in diverse chemical forms, as sediments act as a major sink of metals for the marine system [89, 90]. Moreover, metals specifically iron, can abiotically or biologically undergo oxidation or mobilization at pH above 5, under aerobic, anaerobic or even partially aerobic conditions, especially in temperature that increase dissolution of mineral salts [91, 92].

Research showed that Fenton active metals, especially iron, can catalyze free radical chain reactions in presence of hydrogen peroxide or superoxide anion, which is considered a mechanism for metal induced toxicity (discussed in literature review) [45, 64]. As metal toxicity and resistance are related to and aggravated by Reactive Oxygen Species (ROS), abundance of hydrogen peroxide (H_2O_2) was investigated in brine pools, on genetic basis. Using the PeroxiBase database [82], metagenomes were compared to different DNA sequences of microbial peroxidases in order to examine abundance of genes encoding peroxidases, which probably will give a clue about the level of H_2O_2 in brine water. Peroxidases are oxidoreductases that are crucial for regulation of ROS by catalyzing reduction of hydrogen peroxide and oxidation of other substrates. High accumulation of ROS beyond antioxidants capacity, in any type of cells, may lead to cell toxicity and death [40, 64, 93]. Despite the fact that brine pools are anoxic dark media, while hydrogen peroxide (H_2O_2) is mainly generated as a byproduct of aerobic respiration, enrichment of peroxidases genes was noticed especially in ATII LCL (914 reads-0.08%) and to much less extent in the other samples. Interestingly, it was confirmed that reaction of pyrite with water in anoxic conditions generates H_2O_2, even in dark conditions. The amount of H_2O_2 generated is directly proportional to the surface area of pyrite crystals [94-97]. This reaction had been explained by the unique chemistry of pyrite, as it has sulfur-deficient defects, in which sulfur exists in (-2) oxidation state, in addition to presence of some Ferric ions (Fe^{3+}). Upon water exposure, Fe^{3+} is reduced to Fe^{2+}, where an electron is extracted from H_2O and hydroxyl radicle ($^{\bullet}OH$) is generated. Spontaneously, H_2O_2 is formed by combining 2 hydroxyl radicles (as appears in the following equations) [95, 97].

$$Fe^{3+}(\text{pyrite}) + H_2O \rightarrow Fe^{2+}(\text{pyrite}) + {}^{\bullet}OH + H^{+} \text{ [97]}$$

$$2\ {}^{\bullet}OH \rightarrow H_2O_2 \text{ [97]}$$

This may explain the enrichment of peroxidase genes in ATII, where hydrogen peroxide is generated from pyrite water interaction. Different studies pointed out that ATII-LCL has zero dissolved oxygen [1], while a recent research confirmed that both ATII-LCL and DD brine have the same minute concentration of dissolved oxygen (0.3 µM) [6]. In both cases, there is low probability that hydrogen peroxide was biologically generated in ATII-LCL, especially that abundance of peroxidases genes in ATII-LCL was more than 3 times that in DD (Table 4).

Phylogenetic analysis showed that Firmicutes only existed and dominated in ATII-LCL, and were represented by *Paenibacillus* genus (64.22%). *Paenibacillus* genus includes more than 150 species. Most of *Paenibacillus* spp. are endospore-forming bacteria, aerobic or facultatively anaerobic [98]. Many studies reported the interaction of *Paenibacillus* genus with mineral ores, specifically *Paenibacillus polymyxa*, and described how this bacterium affects the surface chemistry of mineral ores [99-102]. *Paenibacillus polymyxa* is known for the production of extracellular polysaccharide (ECP), extracellular bacterial proteins (EBP) and some organic acids as oxalic, formic, and acetic acids [101, 103]. ECP as siderophores, do not just help in uptake of metal ions needed for bacterial metabolism, but under high metal exposure some bacteria upregulate ECP expression to sequester metal ions in the external environment [34, 104, 105], while in case toxic metals bind to soluble siderphores, bacteria in return control membrane transport by increased efflux or reduced intake of soluble metal bound siderophores [34, 106, 107]. It was reported that ECP adsorption on mineral ores as hematite and corundum, render ores more hydrophilic, which increase dissolution of metal ions from ores [99]. In addition, adsorption of ECP, EBP, and even bacterial cells of *Paenibacillus polymyxa* was observed to be high onto pyrite at different pH, which lead to pyrite flocculation [101]. Consequently, different bacterial species have been utilized in biobeneficiation, in which interaction of microorganisms with mineral ores leads to removal of undesired mineral constituents [99]. Beside iron tolerance, *Paenibacilli* were identified to be resistant to other metals as zinc cadmium and copper [108, 109]. All the above mentioned facts may explain dominance of *Paenibacillus* genus in a highly metalliferous water layer as ATII-LCL and shows that *Paenibacilli* were not just adapted to extreme conditions but they may have induced change in the surrounding medium.

Alteromonas genus (order : Alteromonadales) was also highly abundant in ATII-LCL (15.68%). *Alteromonas* has been isolated before from different marine ecosystems including sea-tidal flats ,deep and surface sea water. Interestingly, *Alteromonas* was described to be copiotrophic as previous studies showed that it can biodegrade, metabolize and grow on aromatic organic compounds available in marine environments. Moreover, a recent study showed that *Alteromonas* strain has been isolated from a unique sea-tidal flats that experience: seasonal oxygen-tension and temperature fluctuation from below 0 ºC till above 30 ºC, in addition to hydrocarbon contaminants [110-112]. Resembling *Paenibacillus*, *Altermonas* showed to be polysaccharide-producing bacteria [110-113]. The observation that both *Paenibacillus* [114-116], *Alteromonas* [112] are aromatic compound degraders, agrees with a recent study confirming availability of aromatic compounds and microbial aromatic compound degradation activity in ATII-LCL [19].

Exclusive bacterial taxa have been detected in ATII-UCL: *Phyllobacterium* (53.96%), *Enhydrobacter* (13.37%), and *SAR406* (10.21%). However, a recent study reported that ATII brine-sea water interface was also dominated by *Phyllobacterium*, beside the abundance of *Enhydrobacter* and *SAR406* [15]. These results are may be explained by contamination from the above layer, especially that the ATII interface is just overlying ATII-UCL.

On the other hand, *Cupriavidus* genus of family *Burkholderiaceae* was abundant in all brine water layers except in DD (Supplementary Table 1). *Cupriavidus* spp., including *Cupriavidus basilensis*, *Cupriavidus campinensis*, and *Cupriavidus metallidurans,* are known to be metal resistant to different metals such as mercury, lead, zinc, copper, cobalt, and cadmium [117-119]. Beside metal resistance, *Cupriavidus* members are capable of degrading and utilizing organic aromatic compounds[120, 121].

Regarding archaeal communities, class Marine Group I (MGI) of *Crenarchaeota,* was detected in both upper (87.31%) and lower (14.46%) convective layers of ATII. Though, the first cultured archaeon of MGI was aerobic and nitrifying, it has been detected in different sea depths up to 3000m below sea surface [122]. Moreover, a recent study on

ATII and DD sediments reported the abundance of MGI in all sediment sections and also in the water column [17]. While *Euryarchaeota*, represented by unassigned genus of family Marine Group II (MGII), were only highly abundant in ATII-LCL (24.84%). Abundance of MGII in ATII-LCL may have been a contamination from overlying layers, as most previous studies detected MGII at upper water layers [123].

Using SEED Subsytems annotation via MG-RAST server [79, 80], we examined the enrichment and abundance of the sets of genes related to microbial metal interaction and resistance. ATII-LCL followed by ATII-UCL showed significantly the highest relative abundance of metal resistance genes, iron metabolism and transport, and metal transporters (Supplementary Table 3,5,6). These results supported both our chemical and phylogenetic analyses. To further validate our results, BacMet database [81] of experimentally confirmed bacterial metal resistance genes, was used for metagenomes annotation. Overall results again correlated with results generated via MG-RAST (Figure 4) [79, 80]. As expected, there were some differences regarding the most enriched genes in the metagenomes. The fact that BacMet database [81]: was small sized (444 genes), included only experimentally confirmed genes, and had different genes than that of SEED database [80], created disparity in results.

In ATII-LCL, cobalt-zinc-cadmium resistance genes were the most abundant resistance genes and were mostly comprised of cobalt-zinc-cadmium resistance proteins CzcA/ CzcB/ CzcC/CzcD (Supplementary Table 3). Czc resistance proteins were highly abundant, most probably because of zinc concentration (3.9 ppm), which was the highest zinc concentration among brine pools. Different Czc proteins together form an efflux system for metals detoxification, which is powered by proton motive force. The efflux system composed of several protein as CzcC which is an outer membrane factor, and CzcB that act as a membrane fusion protein [124].

As copper was only detected in ATII, copper homeostasis and tolerance genes were prominent in ATII-LCL. Copper-translocating P-type ATPases, which showed 2074 reads in ATII-LCL, are members of large family of metal transporting P-type ATPases that is

involved in homeostasis of the ions of soft Lewis acids (Cu^+ ,Hg^+ ,Ag^+, ..etc). Soft metal P-type ATPases have been found in archaea, prokaryotes and eukaryotes [125, 126]. Despite the fact that copper is an essential metal that is incorporated in structure of different oxidoreductases as superoxide dismutase and cytochrome oxidase, excess intracellular copper may cause severe damage. Accordingly, copper transporting pumps as P-type ATPases act on translocating excess Cu from cytosol through extrusion outside the cell or accumulating it into its organelles [125, 126].

As expected, ATII-LCL genes involved in iron metabolism and acquisition were more enriched than DD and KD by more than 4 and 11 times, respectively. The high abundance of ferrichrome-iron receptor genes (322 reads) may be explained by the presence of high iron content and the ECP producing iron resistant *Paenebacillus* genus. Ferrichrome is a hydroxamate that complexes with iron with high affinity. It is one of 500 highly electronegative siderophore types that are produced by gram-positive and gram-negative bacteria [105]. Ferrichrome-iron receptor genes enrichment, may support the idea that extracellular sequestration by siderophores is one of the most utilized iron resistance pathway used by bacterial communities in ATII-LCL.

Regarding metal membrane transporters, ATII-LCL manganese transporter genes were the most enriched, followed by zinc transporters. This may agree with the observation that under H_2O_2 stress, some bacteria increase manganese uptake as a defense mechanism, in order to displace ferrous ions from mononuclear metalloenzymes. Since manganese is not Fenton active metal, the latter action lessen Fenton induced ROS generation, which agrees with the noticed enrichment of genes encoding peroxidases in ATII-LCL [54, 127]. Manganese transporter enrichment also may simply arise just because of the high manganese abundance in ATII-LCL, while high abundance of zinc transporters, low abundance of that of cobalt, high concentration of zinc metal (3.9 ppm) in ATII-LCL, and absence of cadmium and cobalt metals in our samples affirms that most probably cobalt-zinc- cadmium resistance proteins are enriched mainly because of high zinc concentration in ATII-LCL not because of cadmium or cobalt.

4.2. Discovery Deep (DD) and Kebrit Deep (KD)

Although DD sediments are described to be rich and metalliferous, they still proved to be less in metal content than ATII [1]. Unlike ATII, metal content of DD did not reflect on brine water metals concentration except in manganese (Mn) and rubidium (Rb). Those results were also confirmed by the latest study conducted on brine pools, which showed also noticeable increase in DD nitrate and ammonia relative to ATII brine water [6]. Relatively low brine water metal concentration may have derived from different composition of both: DD sediments, and dominant microbial communities that affect dissolution and solubility of metals in water.

DD was dominated mainly by *Gammaproteobacteria* represented by genera: *Halomonas* (43.49%) and *Altermonas* (6.79%). Both genera were also detected in ATII-LCL, which may be attributed to the subsurface connection between the two pools [8]. *Halomonas* genus is one of the genera that have largest number of heterogenous species, which have a unique ability to grow in wide range of salinity. Consequently, *Halomona*s genus is considered as a model for studying halophilism [128]. *Halomonas* members have been isolated from different saline environment including sea water, soils and even salty food. Some of *Halomonas* species can tolerate up to 27% (w/v) salinity, 50 º C temperature and live in pH range of 5-11 [129]. Moreover, some strains have the ability to grow in aneorobic conditions, which clarifies how it tolerates brine pools condition [130].

In DD, uncultured *Thermoplasmata* of the South African Goldmine (SAG) showed highest abundance of 50.82%, followed by unclassified ST-12K10A lineage (27.09%), and unassigned genus of family *Halobacteriaceae* (11.87%). Interestingly, SAG group were also strikingly dominating KD by 96.53%. Uncultured SAG group was first discovered in different water samples from South African goldmines [131]. Most of archaea inhabiting DD brine water as: SAG group, unclassified ST-12K10A lineage, family *Halobacteriaceae* had been detected recently in nitrogen rich subsection in DD sediments [17]. Presence of such archaeal community in nitrogen rich media gives an insight about their metabolism,

especially that DD brine water showed higher concentrations of ammonia and nitrate, relative to ATII [6].

In accordance with chemical and phylogenetic analysis, DD showed less abundance of metal interaction involved genes, when compared to ATII. This was observed in genes encoding: peroxidases, metal resistance, iron metabolism and metal transporters (Figure 4).

Unlike ATII and DD, KD brine water showed excessive abundance of ammonia, sulfate and hydrogen sulfide [6]. Furthermore, KD had been described to have massive amorphous and porous sulfide deposits mainly pyrite and sphalerite [132, 133]. KD sulfide deposits were observed to have distinctive oxidized surface of iron hydroxides and precipitants of sulfides, in addition to the fact that they were tar and asphalt impregnated [133]. Similar to DD, most metals concentrations in KD were low and accordingly did not reflect on enrichment of genes involved in metal interaction or peroxidases synthesis (Figure 4).

Dominance of *Acidovorax* genus (44.07%) together with uncommon presence of amorphous oxidized iron sulfide deposits in KD [6], give a new inference about some biochemical activities taking place in brine water. The facultative anaerobe *Acidovorax* have been known for their ability to couple iron-oxidation to nitrate reduction in anaerobic marine environment to gain energy, and have been identified in iron sulfide-nitrate rich water [134, 135]. Anaerobic bacterial oxidation of iron sulfides coupled to nitrate reduction results in precipitation of ferric hydroxides that are poorly soluble. Accordingly, some iron oxidizing bacteria have been used in biomineralization to clear solutions of soluble metal ions [136]. Other studies showed that precipitation of iron hydroxides also promote co-precipitation of other metals from solutions [137, 138]. This reaction can be summarized by the following equation:

$$10\ FeS_2 + 30\ NO_3^- + 20\ H_2O \rightarrow 10\ Fe(OH)_3 + 15\ N_2 + 10\ H^+ + 20\ SO_4^{2-}$$ [139]

The above reaction can in part explain the presence of insoluble iron hydroxides deposits on pyrite, and low metal water content in KD [133]. Likewise, other bacterial genera as *Dechloromonas* and *Aquabacterium,* which are capable of coupling iron-oxidation to nitrate reduction were detected in KD [134, 140, 141]. *Roseateles* genus was also highly abundant in KD, which is well known for its unique ability to degrade aliphatic polycarbons as poly(e-caprolactone), poly(hexamethylene carbonate), and poly(tetramethylene carbonate) [142, 143] Though Kebrit Deep showed to be rich in different types of hydrocarbons, as alkanes (normal, branched and cyclic), it is not confirmed whether *Roseateles* genus can use such compounds as carbon sources or not [144]. Moreover, previously identified *Roseateles* members were aerobic ones, which suggests that may be it is a new anaerobic species, or a sort of contamination, though it was not detected before in the overlying water layers [15, 145].

Interestingly, hydrogen sulfide was only detected in KD water, showing unusual high concentration (526.7 µM) [6]. High water hydrogen sulfide content may have also contributed in decreasing water metal concentration, as amorphous iron sulfide precipitates out of the reaction of hydrogen sulfide with ferrous iron in water [146]. In addition, huge H_2S content may indicate biogenic H_2S production as a result of bacterial sulfate reduction, which was supported by detection of *Desulfovermiculus* sulfate reducing genus in KD (Supplementary Table 1) [147]. The presence of highly nitrogenous media in KD (ammonia concentration = 2657 µM) [6], may also explain the monopoly of archaeal pyrotags by SAG group (96.53%.), which was identified before in DD nitrogen rich subsurface sediments [17] .

4.3. Arsenite oxidase (ArOx)

Screening our metagenomic libraries showed the presence of different genes encoding metal resistance and detoxifying proteins (Supplementary Table 3,4). Recently, a halotolerant thermostable mercuric reductase enzyme has been isolated and characterized from the same ATII-LCL we are using [74]. Likewise, we identified computationally an

arsenite oxidase (ArOx) enzyme from ATII-LCL, that was proposed to infer bacterial metal resistance, and potentially has an application in metal detoxification [148-150].

Arsenic (As) is present naturally or as a contaminant in different environments like: geothermal springs and industry contaminated areas. Arsenic is known to be extremely toxic in its soluble forms especially in arsenite (As^{3+}) oxidation state, which was reported to be about 100 more toxic than arsenate (As^{5+}) [151]. Arsenite toxicity is mainly attributed to its high affinity to bind dithiols compounds and sulfhydryl groups of proteins, while arsenate which is a phosphate analogue, induce toxicity by replacing phosphate and disrupting cellular phosphorylation processes [148, 152].

In general, bacteria resist toxicity of arsenate and arsenite by either controlling their transport, keeping low intracellular concentrations, or via converting them to relatively less toxic forms. Moreover, some bacteria can methylate arsenite directly, or convert it first to less toxic arsenate before methylation [148]. Though some studies point out that arsenite oxidase (ArOx) has a role in detoxification, others show that some microorganisms can use arsenic compounds as electron donors or electron acceptors using respiratory chains and other redox enzymes [148, 150, 153, 154].

ArOx is composed of two subunits: a large one of about 90– 100 kDa and a small one of about 14 kDa. The large subunit harbors molybdopterin cofactor and [3Fe- 4S] cluster. While the small subunit is a Rieske protein which has [2Fe- 2S] center [152, 154]. ArOX was found to be either associated to cytoplasmic membrane or in the periplasm. It was proposed that oxidation of arsenite starts by the molybdenum center which accepts electron pair from arsenite, followed by the transfer of electrons to neighbor [3Fe-4S] cluster, then [2Fe-2S] of Rieske subunit and finally to the available coupling protein like azurin or cytochrome c [152, 154].

Arsenite oxidase of *Cupriavidus basilensis* showed highest identity with ATII-LCL ArOX. *Cupriavidus basilensis* (formerly *Ralstonia basilensis*) is known to be aerobic metal resistant bacterium that was first isolated from sediments from freshwater close to a

contaminated site [155]. Later it was isolated together with other heavy metal resistant bacteria from an industrial biotope, and was described to grow at range of 4-37 °C [117]. As *C. basilensis* had been described to be an aerobic mesophilic bacterium, it is most probably that we got it as a contamination from less harsh overlying water layers.

Amino acids composition (positively and negatively charged amino acids) (Table 8) that may give an inference about enzyme halophilicity [156, 157], did not show significant difference between ATII-LCL and *C. basilensis* ArOX enzymes. Likewise, salt bridges in *C. basilensis* ArOX showed to be just slightly higher than that of ATII-LCL ArOX, which may indicate comparable thermostability [158]. The latter preliminary results are based on 3D models that were built on available templates of *Alcaligensis faecalis,* which were of low sequences homology (less than 70%) with ATII-LCL sequences. Consequently, these data are not probably very accurate, and experimental isolation, expression, and characterization of the enzyme would show its exact physiochemical properties.

Eventually, several arsenic removal techniques from contaminated water are based on oxidation of arsenite to arsenate chemically, and then precipitating arsenate by alkaline precipitation [151]. But the latter chemical remediation process proved to be costly and polluting [151]. Accordingly, biological oxidation using microbial enzymes shows more efficient way in decontaminating water from arsenic.

5. Conclusion

This study successfully identified free living metal-resistant prokaryotic communities inhabiting brine pools water and highlighted different microbial metal interaction mechanisms that probably take place in such metaliferrous environment. Using 16S rRNA pyrotags, shot-gun 454-pyrosequencing, and chemical profiles, we were able to learn how bacteria tolerate and induce changes to the surrounding environment. Moreover, we were able to show how geochemical conditions shaped the abundance of microbial communities and affected their microbiomes. Interestingly, each of three brine pools (ATII, DD, and KD) showed different versions of microbial-metal interaction. Excessive abundance of dissolved metals in ATII, which was in part promoted by bacterial communities, was reflected mainly on development of metal resistance and oxidative stress. In addition, our analyses showed how prokaryotes use different metal resistance mechanisms, as extracellular sequesteration, efflux pumps, and detoxifying enzymes, especially in ATII. Though DD showed relatively lower metal content than ATII, higher levels of ammonia and nitrate may had affected prokaryotic abundance there. However, KD displayed a totally different pattern of mutual interaction between the environment and microbial communities, where some bacteria were able to take advantage of metal abundance to generate their own energy. Eventually, we give an example of metal detoxifying enzyme that shows how we can make use of metal interaction phenomenon.

6. References

1. Gurvich, E.G., *Metalliferous sediments of the world ocean: fundamental theory of deep-sea hydrothermal sedimentation*. 2006: Springer.
2. Hartmann, M., et al., *Hydrographic structure of brine-filled deeps in the Red Sea—new results from the Shaban, Kebrit, Atlantis II, and Discovery Deep.* Marine Geology, 1998. **144**(4): p. 311-330.
3. Miller, A.R., et al., *Hot brines and recent iron deposits in deeps of the Red Sea.* Geochimica et Cosmochimica Acta, 1966. **30**(3): p. 341-359.
4. Oudin, E., Y. Thisse, and D. Ramboz, *Fluid inclusion and mineralogical evidence for high-temperature saline hydrothermal circulation in the Red Sea metalliferous sediments: Preliminary results.* Mar. Min, 1984. **5**(1): p. 3-31.
5. Antunes, A., D.K. Ngugi, and U. Stingl, *Microbiology of the Red Sea (and other) deep‐sea anoxic brine lakes.* Environmental microbiology reports, 2011. **3**(4): p. 416-433.
6. Ngugi, D.K., et al., *Comparative genomics reveals adaptations of a halotolerant thaumarchaeon in the interfaces of brine pools in the Red Sea.* The ISME journal, 2015. **9**(2): p. 396-411.
7. Hunt, J.M., et al., *Red Sea: detailed survey of hot-brine areas.* Science, 1967. **156**(3774): p. 514-516.
8. Hoffmann, R., *Hot brines in the Red Sea.* American Scientist, 1991. **79**: p. 298-299.
9. Schmidt, M., et al., *High-resolution methane profiles across anoxic brine–seawater boundaries in the Atlantis-II, Discovery, and Kebrit Deeps (Red Sea).* Chemical geology, 2003. **200**(3): p. 359-375.
10. Qian, P.-Y., et al., *Vertical stratification of microbial communities in the Red Sea revealed by 16S rDNA pyrosequencing.* The ISME journal, 2011. **5**(3): p. 507-518.
11. Ferreira, A.J., et al., *Core microbial functional activities in ocean environments revealed by global metagenomic profiling analyses.* PloS one, 2014. **9**(6): p. e97338.
12. Eder, W., et al., *Microbial diversity of the brine-seawater interface of the Kebrit Deep, Red Sea, studied via 16S rRNA gene sequences and cultivation methods.* Applied and environmental microbiology, 2001. **67**(7): p. 3077-3085.
13. Fiala, G., et al., *Flexistipes sinusarabici, a novel genus and species of eubacteria occurring in the Atlantis II Deep brines of the Red Sea.* Archives of Microbiology, 1990. **154**(2): p. 120-126.
14. Trüper, H.G., J.J. Kelleher, and H.W. Jannasch, *Isolation and characterization of sulfate-reducing bacteria from various marine environments.* Archiv für Mikrobiologie, 1969. **65**(3): p. 208-217.
15. Abdallah, R.Z., et al., *Aerobic methanotrophic communities at the Red Sea brine-seawater interface.* Frontiers in microbiology, 2014. **5**.
16. Eder, W., W. Ludwig, and R. Huber, *Novel 16S rRNA gene sequences retrieved from highly saline brine sediments of Kebrit Deep, Red Sea.* Archives of microbiology, 1999. **172**(4): p. 213-218.

17. Siam, R., et al., *Unique prokaryotic consortia in geochemically distinct sediments from Red Sea Atlantis II and Discovery Deep brine pools.* PloS one, 2012. **7**(8): p. e42872.
18. Bougouffa, S., et al., *Distinctive microbial community structure in highly stratified deep-sea brine water columns.* Applied and environmental microbiology, 2013. **79**(11): p. 3425-3437.
19. Wang, Y., et al., *Hydrothermally generated aromatic compounds are consumed by bacteria colonizing in Atlantis II Deep of the Red Sea.* The ISME journal, 2011. **5**(10): p. 1652-1659.
20. Wang, Y., et al., *Autotrophic microbe metagenomes and metabolic pathways differentiate adjacent Red Sea brine pools.* Scientific reports, 2013. **3**.
21. Watson, S.W. and J.B. Waterbury, *The sterile hot brines of the Red Sea*, in *Hot brines and recent heavy metal deposits in the Red Sea*. 1969, Springer. p. 272-281.
22. Nies, D.H., *Microbial heavy-metal resistance.* Applied microbiology and biotechnology, 1999. **51**(6): p. 730-750.
23. Lemire, J.A., J.J. Harrison, and R.J. Turner, *Antimicrobial activity of metals: mechanisms, molecular targets and applications.* Nature Reviews Microbiology, 2013. **11**(6): p. 371-384.
24. Valko, M., H. Morris, and M. Cronin, *Metals, toxicity and oxidative stress.* Current medicinal chemistry, 2005. **12**(10): p. 1161-1208.
25. Harrison, J.J., et al., *Copper and quaternary ammonium cations exert synergistic bactericidal and antibiofilm activity against Pseudomonas aeruginosa.* Antimicrobial agents and chemotherapy, 2008. **52**(8): p. 2870-2881.
26. Clarkson, T., *Molecular and ionic mimicry of toxic metals.* Annual review of pharmacology and toxicology, 1993. **33**(1): p. 545-571.
27. Haas, K.L. and K.J. Franz, *Application of metal coordination chemistry to explore and manipulate cell biology.* Chemical reviews, 2009. **109**(10): p. 4921-4960.
28. Pearson, R.G., *Hard and soft acids and bases.* Journal of the American Chemical Society, 1963. **85**(22): p. 3533-3539.
29. Parr, R.G. and R.G. Pearson, *Absolute hardness: companion parameter to absolute electronegativity.* Journal of the American Chemical Society, 1983. **105**(26): p. 7512-7516.
30. Stohs, S. and D. Bagchi, *Oxidative mechanisms in the toxicity of metal ions.* Free Radical Biology and Medicine, 1995. **18**(2): p. 321-336.
31. Finney, L.A. and T.V. O'Halloran, *Transition metal speciation in the cell: insights from the chemistry of metal ion receptors.* Science, 2003. **300**(5621): p. 931-936.
32. Nies, D.H., *Efflux-mediated heavy metal resistance in prokaryotes.* FEMS microbiology reviews, 2003. **27**(2-3): p. 313-339.
33. Williams, J.W. and S. Silver, *Bacterial resistance and detoxification of heavy metals.* Enzyme and microbial technology, 1984. **6**(12): p. 530-537.
34. Schalk, I.J., M. Hannauer, and A. Braud, *New roles for bacterial siderophores in metal transport and tolerance.* Environmental microbiology, 2011. **13**(11): p. 2844-2854.
35. Lemire, J., et al., *Pseudomonas fluorescens orchestrates a fine metabolic-balancing act to counter aluminium toxicity.* Environmental microbiology, 2010. **12**(6): p. 1384-1390.

36. Silver, S. and L.T. Phung, *Bacterial heavy metal resistance: new surprises.* Annual Reviews in Microbiology, 1996. **50**(1): p. 753-789.
37. Silver, S. and L. Phung, *Heavy metals, bacterial resistance.* Encyclopedia of microbiology, 2009: p. 220-227.
38. Harrison, J.J., et al., *Chromosomal antioxidant genes have metal ion-specific roles as determinants of bacterial metal tolerance.* Environmental microbiology, 2009. **11**(10): p. 2491-2509.
39. Nunoshiba, T., et al., *Role of iron and superoxide for generation of hydroxyl radical, oxidative DNA lesions, and mutagenesis in Escherichia coli.* Journal of Biological Chemistry, 1999. **274**(49): p. 34832-34837.
40. Touati, D., et al., *Lethal oxidative damage and mutagenesis are generated by iron in delta fur mutants of Escherichia coli: protective role of superoxide dismutase.* Journal of bacteriology, 1995. **177**(9): p. 2305-2314.
41. Itoh, M., et al., *Mechanism of chromium (VI) toxicity in Escherichia coli: is hydrogen peroxide essential in Cr (VI) toxicity?* Journal of biochemistry, 1995. **117**(4): p. 780-786.
42. Macomber, L., C. Rensing, and J.A. Imlay, *Intracellular copper does not catalyze the formation of oxidative DNA damage in Escherichia coli.* Journal of bacteriology, 2007. **189**(5): p. 1616-1626.
43. Neyens, E. and J. Baeyens, *A review of classic Fenton's peroxidation as an advanced oxidation technique.* Journal of Hazardous materials, 2003. **98**(1): p. 33-50.
44. Imlay, J.A., *Pathways of oxidative damage.* Annual Reviews in Microbiology, 2003. **57**(1): p. 395-418.
45. Strlič, M., et al., *A comparative study of several transition metals in Fenton-like reaction systems at circum-neutral pH.* Acta Chim Slov, 2003. **50**(4): p. 619-632.
46. Geslin, C., et al., *The manganese and iron superoxide dismutases protect Escherichia coli from heavy metal toxicity.* Research in microbiology, 2001. **152**(10): p. 901-905.
47. Barnese, K., et al., *Biologically relevant mechanism for catalytic superoxide removal by simple manganese compounds.* Proceedings of the National Academy of Sciences, 2012. **109**(18): p. 6892-6897.
48. Macomber, L. and J.A. Imlay, *The iron-sulfur clusters of dehydratases are primary intracellular targets of copper toxicity.* Proceedings of the National Academy of Sciences, 2009. **106**(20): p. 8344-8349.
49. Xu, F.F. and J.A. Imlay, *Silver (I), mercury (II), cadmium (II), and zinc (II) target exposed enzymic iron-sulfur clusters when they toxify Escherichia coli.* Applied and environmental microbiology, 2012. **78**(10): p. 3614-3621.
50. Helbig, K., C. Grosse, and D.H. Nies, *Cadmium toxicity in glutathione mutants of Escherichia coli.* Journal of bacteriology, 2008. **190**(15): p. 5439-5454.
51. Helbig, K., et al., *Glutathione and transition-metal homeostasis in Escherichia coli.* Journal of bacteriology, 2008. **190**(15): p. 5431-5438.
52. Stadtman, E., *Oxidation of free amino acids and amino acid residues in proteins by radiolysis and by metal-catalyzed reactions.* Annual review of biochemistry, 1993. **62**(1): p. 797-821.

53. Stadtman, E. and R. Levine, *Free radical-mediated oxidation of free amino acids and amino acid residues in proteins.* Amino acids, 2003. **25**(3-4): p. 207-218.
54. Anjem, A. and J.A. Imlay, *Mononuclear iron enzymes are primary targets of hydrogen peroxide stress.* Journal of Biological Chemistry, 2012. **287**(19): p. 15544-15556.
55. Calderón, I.L., et al., *Tellurite-mediated disabling of [4Fe–4S] clusters of Escherichia coli dehydratases.* Microbiology, 2009. **155**(6): p. 1840-1846.
56. Ogunseitan, O., S. Yang, and J. Ericson, *Microbial δ-aminolevulinate dehydratase as a biosensor of lead bioavailability in contaminated environments.* Soil Biology and Biochemistry, 2000. **32**(13): p. 1899-1906.
57. Macomber, L., S.P. Elsey, and R.P. Hausinger, *Fructose-1, 6-bisphosphate aldolase (class II) is the primary site of nickel toxicity in Escherichia coli.* Molecular microbiology, 2011. **82**(5): p. 1291-1300.
58. Feng, Q., et al., *A mechanistic study of the antibacterial effect of silver ions on Escherichia coli and Staphylococcus aureus.* Journal of biomedical materials research, 2001(52): p. 662-8.
59. Holt, K.B. and A.J. Bard, *Interaction of silver (I) ions with the respiratory chain of Escherichia coli: an electrochemical and scanning electrochemical microscopy study of the antimicrobial mechanism of micromolar Ag+*. Biochemistry, 2005. **44**(39): p. 13214-13223.
60. Dibrov, P., et al., *Chemiosmotic mechanism of antimicrobial activity of Ag+ in Vibrio cholerae.* Antimicrobial agents and chemotherapy, 2002. **46**(8): p. 2668-2670.
61. Hong, R., et al., *Membrane lipid peroxidation in copper alloy-mediated contact killing of Escherichia coli.* Applied and environmental microbiology, 2012. **78**(6): p. 1776-1784.
62. Kaneko, Y., et al., *The transition metal gallium disrupts Pseudomonas aeruginosa iron metabolism and has antimicrobial and antibiofilm activity.* The Journal of clinical investigation, 2007. **117**(4): p. 877.
63. Keyer, K. and J.A. Imlay, *Superoxide accelerates DNA damage by elevating free-iron levels.* Proceedings of the National Academy of Sciences, 1996. **93**(24): p. 13635-13640.
64. Imlay, J.A., S.M. Chin, and S. Linn, *Toxic DNA damage by hydrogen peroxide through the Fenton reaction in vivo and in vitro.* Science, 1988. **240**(4852): p. 640-642.
65. Nishioka, H., *Mutagenic activities of metal compounds in bacteria.* Mutation Research/Environmental Mutagenesis and Related Subjects, 1975. **31**(3): p. 185-189.
66. Wong, P., *Mutagenicity of heavy metals.* Bulletin of environmental contamination and toxicology, 1988. **40**(4): p. 597-603.
67. Handelsman, J., *Metagenomics: application of genomics to uncultured microorganisms.* Microbiology and molecular biology reviews, 2004. **68**(4): p. 669-685.
68. Kennedy, J., et al., *Marine metagenomics: new tools for the study and exploitation of marine microbial metabolism.* Marine drugs, 2010. **8**(3): p. 608-628.
69. Handelsman, J., et al., *Molecular biological access to the chemistry of unknown soil microbes: a new frontier for natural products.* Chemistry & biology, 1998. **5**(10): p. R245-R249.

70. Kircher, M. and J. Kelso, *High-throughput DNA sequencing–concepts and limitations.* Bioessays, 2010. **32**(6): p. 524-536.
71. Temperton, B. and S.J. Giovannoni, *Metagenomics: microbial diversity through a scratched lens.* Current opinion in microbiology, 2012. **15**(5): p. 605-612.
72. Kerkhof, L.J. and R.M. Goodman, *Ocean microbial metagenomics.* Deep Sea Research Part II: Topical Studies in Oceanography, 2009. **56**(19): p. 1824-1829.
73. Mohamed, Y.M., et al., *Isolation and characterization of a heavy metal-resistant, thermophilic esterase from a Red Sea Brine Pool.* Scientific reports, 2013. **3**.
74. Sayed, A., et al., *A novel mercuric reductase from the unique deep brine environment of Atlantis II in the Red Sea.* Journal of Biological Chemistry, 2014. **289**(3): p. 1675-1687.
75. Rusch, D.B., et al., *The Sorcerer II global ocean sampling expedition: northwest Atlantic through eastern tropical Pacific.* PLoS biology, 2007. **5**(3): p. e77.
76. Huse, S.M., et al., *VAMPS: a website for visualization and analysis of microbial population structures.* BMC bioinformatics, 2014. **15**(1): p. 41.
77. Fisher, R.A., *Statistical methods for research workers*, in *Statistical methods for research workers*. 1970, Oliver & Boyd.
78. Team, R.C., *R: A language and environment for statistical computing. R Foundation for Statistical Computing, Vienna, Austria, 2012*. 2012, ISBN 3-900051-07-0.
79. Meyer, F., et al., *The metagenomics RAST server–a public resource for the automatic phylogenetic and functional analysis of metagenomes.* BMC bioinformatics, 2008. **9**(1): p. 386.
80. Aziz, R.K., et al., *The RAST Server: rapid annotations using subsystems technology.* BMC genomics, 2008. **9**(1): p. 75.
81. Pal, C., et al., *BacMet: antibacterial biocide and metal resistance genes database.* Nucleic acids research, 2014. **42**(D1): p. D737-D743.
82. Fawal, N., et al., *PeroxiBase: a database for large-scale evolutionary analysis of peroxidases.* Nucleic acids research, 2013. **41**(D1): p. D441-D444.
83. Scheer, M., et al., *BRENDA, the enzyme information system in 2011.* Nucleic acids research, 2010: p. gkq1089.
84. Marchler-Bauer, A., et al., *CDD: a Conserved Domain Database for the functional annotation of proteins.* Nucleic acids research, 2011. **39**(suppl 1): p. D225-D229.
85. Schwede, T., et al., *SWISS-MODEL: an automated protein homology-modeling server.* Nucleic acids research, 2003. **31**(13): p. 3381-3385.
86. Gille, C. and C. Frömmel, *STRAP: editor for STRuctural Alignments of Proteins.* Bioinformatics, 2001. **17**(4): p. 377-378.
87. Hannington, M.D., C.D. de Ronde, and S. Petersen, *Sea-floor tectonics and submarine hydrothermal systems.* 2005.
88. Bertram, C., et al., *Metalliferous sediments in the Atlantis II Deep—Assessing the geological and economic resource potential and legal constraints.* Resources Policy, 2011. **36**(4): p. 315-329.
89. Uroz, S., et al., *Mineral weathering by bacteria: ecology, actors and mechanisms.* Trends in microbiology, 2009. **17**(8): p. 378-387.
90. Gadd, G.M., *Metals, minerals and microbes: geomicrobiology and bioremediation.* Microbiology, 2010. **156**(3): p. 609-643.

91. Ehrlich, H., *Microbes and metals.* Applied Microbiology and Biotechnology, 1997. **48**(6): p. 687-692.
92. Ehrlich, H.L. and D.K. Newman, *Geomicrobiology*. 2008: CRC press.
93. Linley, E., et al., *Use of hydrogen peroxide as a biocide: new consideration of its mechanisms of biocidal action.* Journal of antimicrobial chemotherapy, 2012. **67**(7): p. 1589-1596.
94. Borda, M.J., et al., *Pyrite-induced hydrogen peroxide formation as a driving force in the evolution of photosynthetic organisms on an early Earth.* Astrobiology, 2001. **1**(3): p. 283-288.
95. Borda, M.J., et al., *A mechanism for the production of hydroxyl radical at surface defect sites on pyrite.* Geochimica et Cosmochimica Acta, 2003. **67**(5): p. 935-939.
96. Cohn, C.A., M.J. Borda, and M.A. Schoonen, *RNA decomposition by pyrite-induced radicals and possible role of lipids during the emergence of life.* Earth and Planetary Science Letters, 2004. **225**(3): p. 271-278.
97. Cohn, C.A., et al., *Pyrite-induced hydroxyl radical formation and its effect on nucleic acids.* Geochemical Transactions, 2006. **7**(3): p. 1-11.
98. Zhu, J., et al., *Paenibacillus wulumuqiensis sp. nov. and Paenibacillus dauci sp. nov., two novel species of the genus Paenibacillus.* Archives of microbiology, 2015: p. 1-7.
99. Deo, N. and K. Natarajan, *Studies on interaction of Paenibacillus polymyxa with iron ore minerals in relation to beneficiation.* International Journal of Mineral Processing, 1998. **55**(1): p. 41-60.
100. Sharma, P. and H. Rao, *Role of a heterotrophic Paenibacillus polymyxa bacteria in the bioflotation of some sulfide minerals.* Mineral biotechnology: microbial aspects of mineral beneficiation, metal extraction, and environmental control, 2001.
101. Patra, P. and K. Natarajan, *Surface chemical studies on selective separation of pyrite and galena in the presence of bacterial cells and metabolic products of Paenibacillus polymyxa.* Journal of Colloid and interface Science, 2006. **298**(2): p. 720-729.
102. Patra, P. and K. Natarajan, *Microbially-induced flocculation and flotation for pyrite separation from oxide gangue minerals.* Minerals Engineering, 2003. **16**(10): p. 965-973.
103. Patra, P. and K. Natarajan, *Microbially induced flotation and flocculation of pyrite and sphalerite.* Colloids and Surfaces B: Biointerfaces, 2004. **36**(2): p. 91-99.
104. Köster, W., *ABC transporter-mediated uptake of iron, siderophores, heme and vitamin B 12.* Research in microbiology, 2001. **152**(3): p. 291-301.
105. Wandersman, C. and P. Delepelaire, *Bacterial iron sources: from siderophores to hemophores.* Annu. Rev. Microbiol., 2004. **58**: p. 611-647.
106. Dimkpa, C.O., et al., *Involvement of siderophores in the reduction of metal-induced inhibition of auxin synthesis in Streptomyces spp.* Chemosphere, 2008. **74**(1): p. 19-25.
107. Hannauer, M., et al., *The PvdRT-OpmQ efflux pump controls the metal selectivity of the iron uptake pathway mediated by the siderophore pyoverdine in Pseudomonas aeruginosa.* Environmental microbiology, 2012. **14**(7): p. 1696-1708.
108. Abou-Shanab, R., P. Van Berkum, and J. Angle, *Heavy metal resistance and genotypic analysis of metal resistance genes in gram-positive and gram-negative*

bacteria present in Ni-rich serpentine soil and in the rhizosphere of Alyssum murale. Chemosphere, 2007. **68**(2): p. 360-367.
109. Rathnayake, I., et al., *Tolerance of heavy metals by gram positive soil bacteria*. 2009, World Academy of Science Engineering and Technology.
110. Semple, K. and D. Westlake, *Characterization of iron-reducing Alteromonas putrefaciens strains from oil field fluids.* Canadian journal of microbiology, 1987. **33**(5): p. 366-371.
111. Raguénès, G., et al., *Alteromonas infernus sp. nov., a new polysaccharide-producing bacterium isolated from a deep-sea hydrothermal vent.* Journal of applied microbiology, 1997. **82**(4): p. 422-430.
112. Math, R.K., et al., *Comparative genomics reveals adaptation by Alteromonas sp. SN2 to marine tidal-flat conditions: cold tolerance and aromatic hydrocarbon metabolism.* PLoS One, 2012. **7**(4): p. e35784.
113. Raguenes, G., et al., *Description of a new polymer-secreting bacterium from a deep-sea hydrothermal vent, Alteromonas macleodii subsp. fijiensis, and preliminary characterization of the polymer.* Applied and environmental microbiology, 1996. **62**(1): p. 67-73.
114. Daane, L., et al., *PAH-degradation by Paenibacillus spp. and description of Paenibacillus naphthalenovorans sp. nov., a naphthalene-degrading bacterium from the rhizosphere of salt marsh plants.* International journal of systematic and evolutionary microbiology, 2002. **52**(1): p. 131-139.
115. Sakai, M., et al., *Isolation and characterization of a novel polychlorinated biphenyl-degrading bacterium, Paenibacillus sp. KBC101.* Applied microbiology and biotechnology, 2005. **68**(1): p. 111-116.
116. Daane, L., et al., *Isolation and characterization of polycyclic aromatic hydrocarbon-degrading bacteria associated with the rhizosphere of salt marsh plants.* Applied and Environmental Microbiology, 2001. **67**(6): p. 2683-2691.
117. Goris, J., et al., *Classification of metal-resistant bacteria from industrial biotopes as Ralstonia campinensis sp. nov., Ralstonia metallidurans sp. nov. and Ralstonia basilensis Steinle et al. 1998 emend.* International journal of systematic and evolutionary microbiology, 2001. **51**(5): p. 1773-1782.
118. Reith, F., et al., *Mechanisms of gold biomineralization in the bacterium Cupriavidus metallidurans.* Proceedings of the National Academy of Sciences, 2009. **106**(42): p. 17757-17762.
119. Mergeay, M. and R. Van Houdt, *Adaptation to Xenobiotics and Toxic Compounds by Cupriavidus and Ralstonia with Special Reference to Cupriavidus metallidurans CH34 and Mobile Genetic Elements*, in *Biodegradative Bacteria*. 2014, Springer. p. 105-127.
120. Perez-Pantoja, D., et al., *Metabolic reconstruction of aromatic compounds degradation from the genome of the amazing pollutant-degrading bacterium Cupriavidus necator JMP134.* FEMS microbiology reviews, 2008. **32**(5): p. 736-794.
121. Lykidis, A., et al., *The complete multipartite genome sequence of Cupriavidus necator JMP134, a versatile pollutant degrader.* PLoS One, 2010. **5**(3): p. e9729.
122. Teske, A. and K.B. Sørensen, *Uncultured archaea in deep marine subsurface sediments: have we caught them all?* The ISME Journal, 2008. **2**(1): p. 3-18.

123. DeLong, E.F., *Archaeal mysteries of the deep revealed.* Proceedings of the National Academy of Sciences, 2006. **103**(17): p. 6417-6418.
124. Intorne, A.C., et al., *Essential role of the czc determinant for cadmium, cobalt and zinc resistance in Gluconacetobacter diazotrophicus PAl 5.* International Microbiology, 2012. **15**(2): p. 69-78.
125. Rensing, C., et al., *CopA: an Escherichia coli Cu (I)-translocating P-type ATPase.* Proceedings of the National Academy of Sciences, 2000. **97**(2): p. 652-656.
126. Rensing, C., M. Ghosh, and B.P. Rosen, *Families of soft-metal-ion-transporting ATPases.* Journal of bacteriology, 1999. **181**(19): p. 5891-5897.
127. Anjem, A., S. Varghese, and J.A. Imlay, *Manganese import is a key element of the OxyR response to hydrogen peroxide in Escherichia coli.* Molecular microbiology, 2009. **72**(4): p. 844-858.
128. Ventosa, A., J.J. Nieto, and A. Oren, *Biology of moderately halophilic aerobic bacteria.* Microbiology and Molecular Biology Reviews, 1998. **62**(2): p. 504-544.
129. Arahal, D.R. and A. Ventosa, *The family Halomonadaceae*, in *The prokaryotes*. 2006, Springer. p. 811-835.
130. Maskow, T. and W. Babel, *Thermokinetic description of anaerobic growth of Halomonas halodenitrificans using a static microcalorimetric ampoule technique.* Journal of Biotechnology, 2003. **101**(3): p. 267-274.
131. Takai, K., et al., *Archaeal diversity in waters from deep South African gold mines.* Applied and Environmental Microbiology, 2001. **67**(12): p. 5750-5760.
132. Scholten, J., et al., *Hydrothermal mineralization in the Red Sea.* Handbook of marine mineral deposits. CRC Press, Boca Raton, Fla, 1999: p. 369-395.
133. Blum, N. and H. Puchelt, *Sedimentary-hosted polymetallic massive sulfide deposits of the Kebrit and Shaban Deeps, Red Sea.* Mineralium Deposita, 1991. **26**(3): p. 217-227.
134. Straub, K.L., et al., *Diversity of ferrous iron-oxidizing, nitrate-reducing bacteria and their involvement in oxygen-independent iron cycling.* Geomicrobiology Journal, 2004. **21**(6): p. 371-378.
135. Haaijer, S.C., et al., *Anoxic iron cycling bacteria from an iron sulfide-and nitrate-rich freshwater environment.* Frontiers in microbiology, 2012. **3**.
136. Miot, J., et al., *Iron biomineralization by anaerobic neutrophilic iron-oxidizing bacteria.* Geochimica et Cosmochimica Acta, 2009. **73**(3): p. 696-711.
137. Hohmann, C., et al., *Anaerobic Fe (II)-oxidizing bacteria show As resistance and immobilize As during Fe (III) mineral precipitation.* Environmental science & technology, 2009. **44**(1): p. 94-101.
138. Dippon, U., et al., *Potential function of added minerals as nucleation sites and effect of humic substances on mineral formation by the nitrate-reducing Fe (II)-oxidizer Acidovorax sp. BoFeN1.* Environmental science & technology, 2012. **46**(12): p. 6556-6565.
139. Hayakawa, A., et al., *Nitrate reduction coupled with pyrite oxidation in the surface sediments of a sulfide-rich ecosystem.* Journal of Geophysical Research: Biogeosciences, 2013. **118**(2): p. 639-649.
140. Chakraborty, A. and F. Picardal, *Induction of nitrate-dependent Fe (II) oxidation by Fe (II) in Dechloromonas sp. strain UWNR4 and Acidovorax sp. strain 2AN.* Applied and environmental microbiology, 2013. **79**(2): p. 748-752.

141. Chakraborty, A. and F. Picardal, *Neutrophilic, nitrate-dependent, Fe (II) oxidation by a Dechloromonas species.* World Journal of Microbiology and Biotechnology, 2013. **29**(4): p. 617-623.
142. Garrity, G.M., J.A. Bell, and T. Lilburn, *Class II. Betaproteobacteria class. nov*, in *Bergey's manual® of systematic bacteriology*. 2005, Springer. p. 575-922.
143. Suyama, T., et al., *Roseateles depolymerans gen. nov., sp. nov., a new bacteriochlorophyll a-containing obligate aerobe belonging to the β-subclass of the Proteobacteria.* International journal of systematic bacteriology, 1999. **49**(2): p. 449-457.
144. Michaelis, W., A. Jenisch, and H.H. Richnow, *Hydrothermal petroleum generation in Red Sea sediments from the Kebrit and Shaban Deeps.* Applied Geochemistry, 1990. **5**(1): p. 103-114.
145. Tringe, S.G., et al., *Comparative metagenomics of microbial communities.* Science, 2005. **308**(5721): p. 554-557.
146. Morse, J.W., et al., *The chemistry of the hydrogen sulfide and iron sulfide systems in natural waters.* Earth-Science Reviews, 1987. **24**(1): p. 1-42.
147. Belyakova, E., et al., *The new facultatively chemolithoautotrophic, moderately halophilic, sulfate-reducing bacterium Desulfovermiculus halophilus gen. nov., sp. nov., isolated from an oil field.* Microbiology, 2006. **75**(2): p. 161-171.
148. Anderson, G., J. Williams, and R. Hille, *The purification and characterization of arsenite oxidase from Alcaligenes faecalis, a molybdenum-containing hydroxylase.* Journal of Biological Chemistry, 1992. **267**(33): p. 23674-23682.
149. Ellis, P.J., et al., *Crystal structure of the 100 kDa arsenite oxidase from Alcaligenes faecalis in two crystal forms at 1.64 Å and 2.03 Å.* Structure, 2001. **9**(2): p. 125-132.
150. Chang, J.-S., et al., *Arsenic detoxification potential of aox genes in arsenite-oxidizing bacteria isolated from natural and constructed wetlands in the Republic of Korea.* Environmental geochemistry and health, 2010. **32**(2): p. 95-105.
151. Muller, D., et al., *Arsenite oxidase aox genes from a metal-resistant β-proteobacterium.* Journal of bacteriology, 2003. **185**(1): p. 135-141.
152. Lieutaud, A., et al., *Arsenite Oxidase from Ralstonia sp. 22 CHARACTERIZATION OF THE ENZYME AND ITS INTERACTION WITH SOLUBLE CYTOCHROMES.* Journal of Biological Chemistry, 2010. **285**(27): p. 20433-20441.
153. Lebrun, E., et al., *Arsenite oxidase, an ancient bioenergetic enzyme.* Molecular biology and evolution, 2003. **20**(5): p. 686-693.
154. Silver, S. and L.T. Phung, *Genes and enzymes involved in bacterial oxidation and reduction of inorganic arsenic.* Applied and Environmental Microbiology, 2005. **71**(2): p. 599-608.
155. Steinle, P., et al., *Aerobic mineralization of 2, 6-dichlorophenol by Ralstonia sp. strain RK1.* Applied and environmental microbiology, 1998. **64**(7): p. 2566-2571.
156. Mevarech, M., F. Frolow, and L.M. Gloss, *Halophilic enzymes: proteins with a grain of salt.* Biophysical chemistry, 2000. **86**(2): p. 155-164.
157. Fukuchi, S., et al., *Unique amino acid composition of proteins in halophilic bacteria.* Journal of molecular biology, 2003. **327**(2): p. 347-357.
158. Kumar, S., C.-J. Tsai, and R. Nussinov, *Factors enhancing protein thermostability.* Protein Engineering, 2000. **13**(3): p. 179-191.

7. Figures

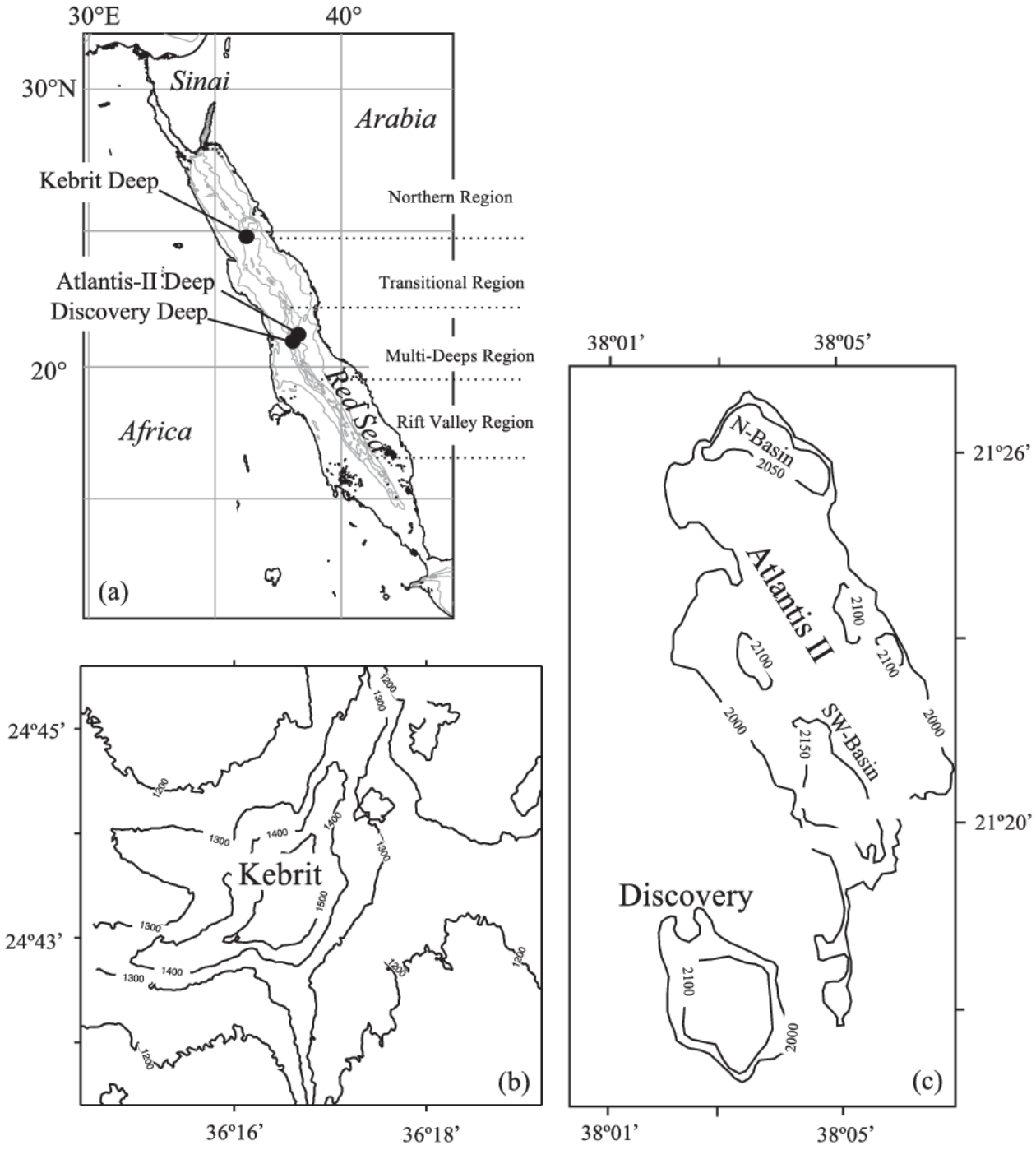

Figure 1. Locations, depth range and shapes of the three studied brine pools, adapted from [9].

(a) Locations of Atlantis II Deep, Discovery Deep, and Kebrit Deep brine pools within the Red Sea. (b) General shape and depth range within Kebrit Deep. (c) General shape and depth range within Atlantis II Deep and Discovery Deep.

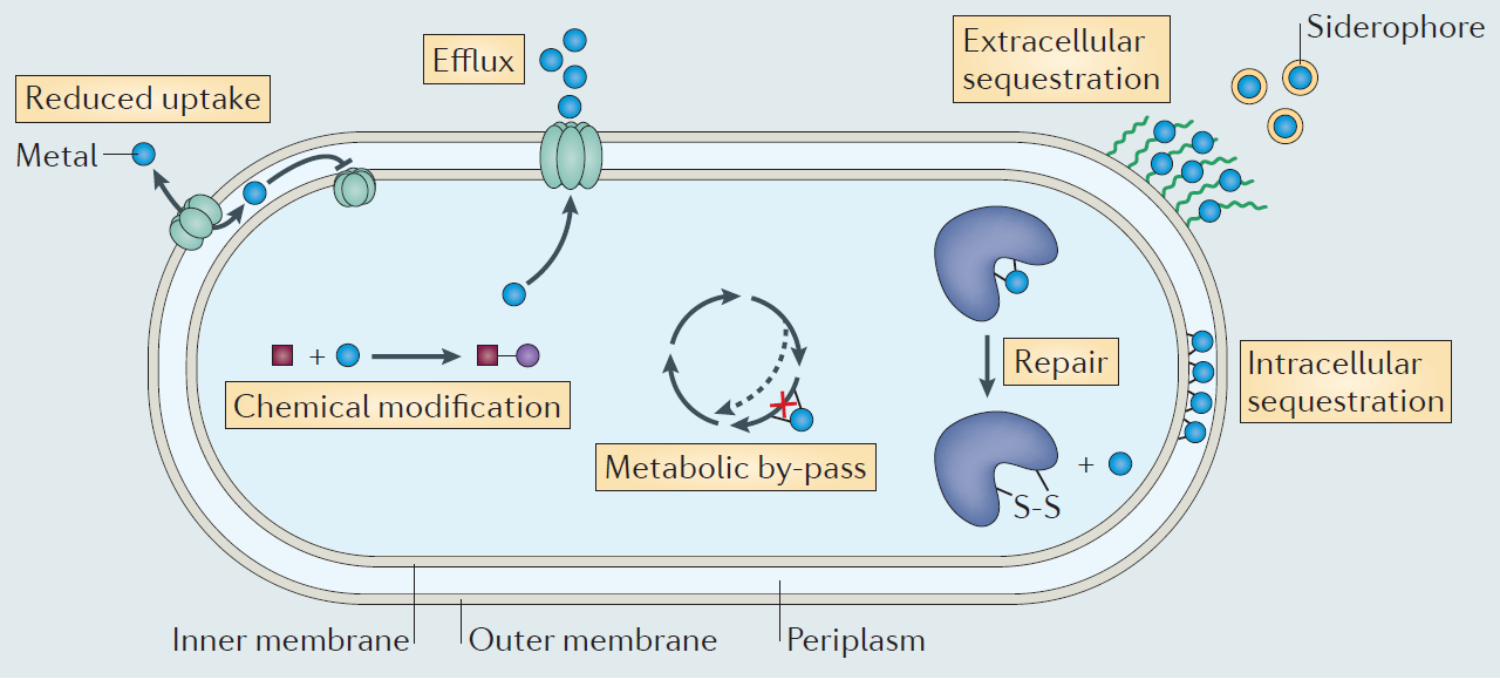

Figure 2. Different mechanisms of metal resistance in prokaryotes, adapted from [23].

General mechanisms of metal resistance in prokaryotes include; control of metals' transport across bacterial membranes (metal efflux and reduced uptake), metals sequestration (intracellular and extracellular sequestration), metabolic by-pass, redox of chemical modification of metals (detoxifying enzymes).

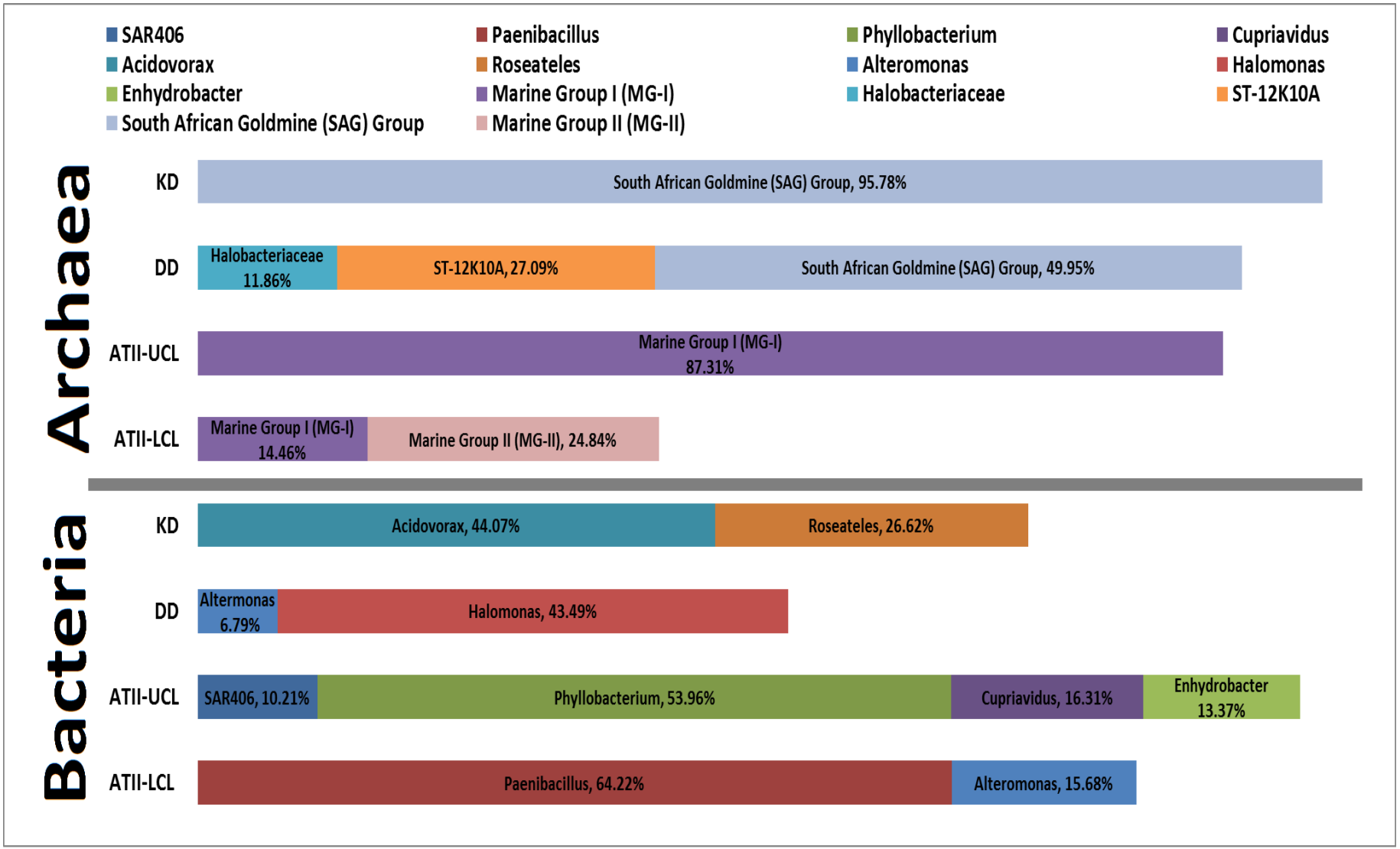

Figure 3. Taxonomic assignment of significant highly abundant OTUs (relative abundance ≥ 5%)to major bacterial and archaeal groups (Genus/last identified taxa level) obtained from brine pools' water.

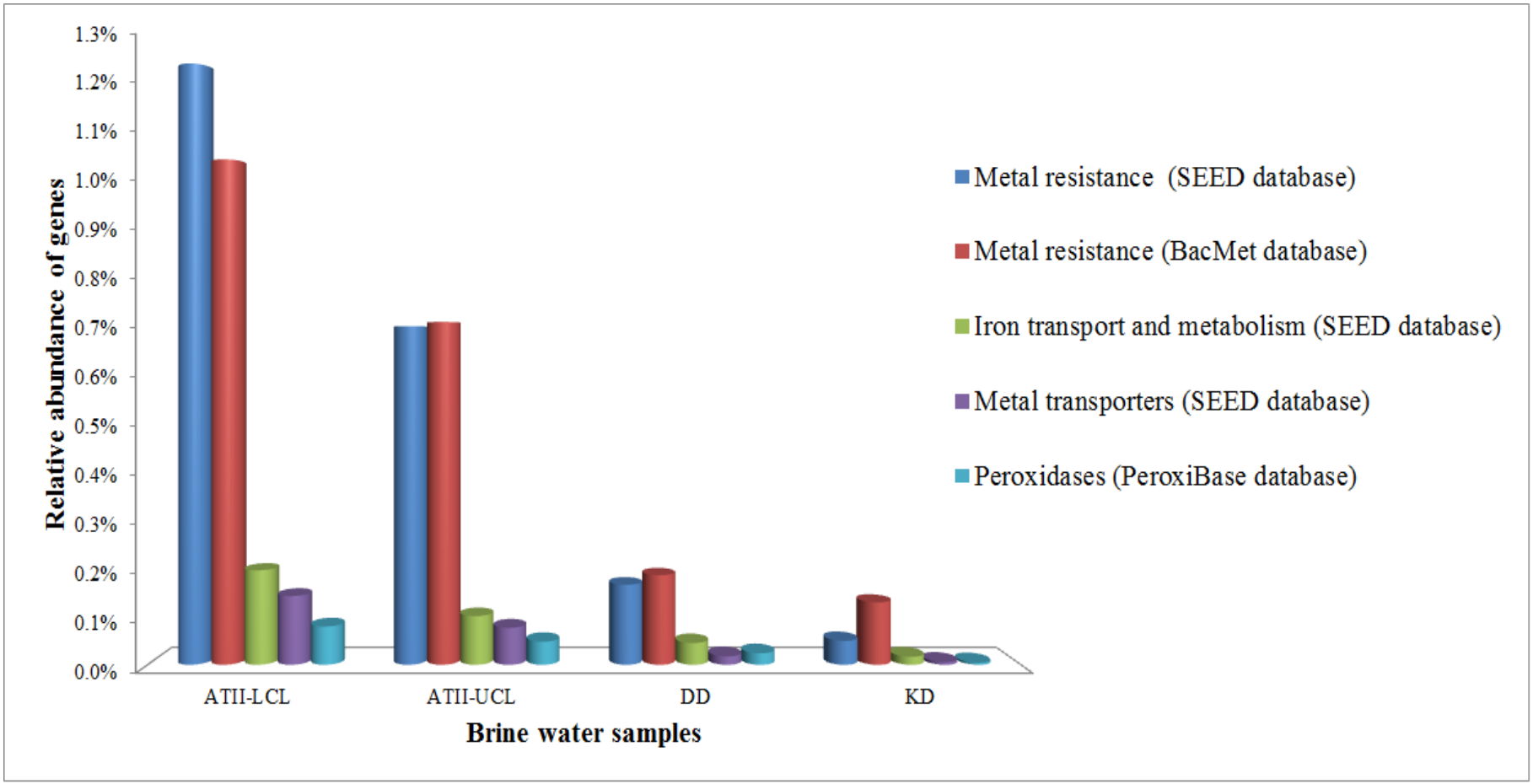

Figure 4. Comparison between ATII-LCL, ATII-UCL, DD, and KD brine water samples, in terms of relative abundance of genes involved in; mental resistance, iron metabolism/transport, membrane metal transport, and encoding peroxidases.

Annotation using SEED database was done via MG-RAST server [80], while annotation of;genes encoding peroxidases by PeroxiBase database [82], and metal resistance genes by BacMet database [81] was done via BLASTx. The same E-value cutoff ($1e^{-5}$) was used for all annotation processes (discussed in Mateials and Methods). Relative abundance of genes is normalized to total number of sequences within each metagenome.

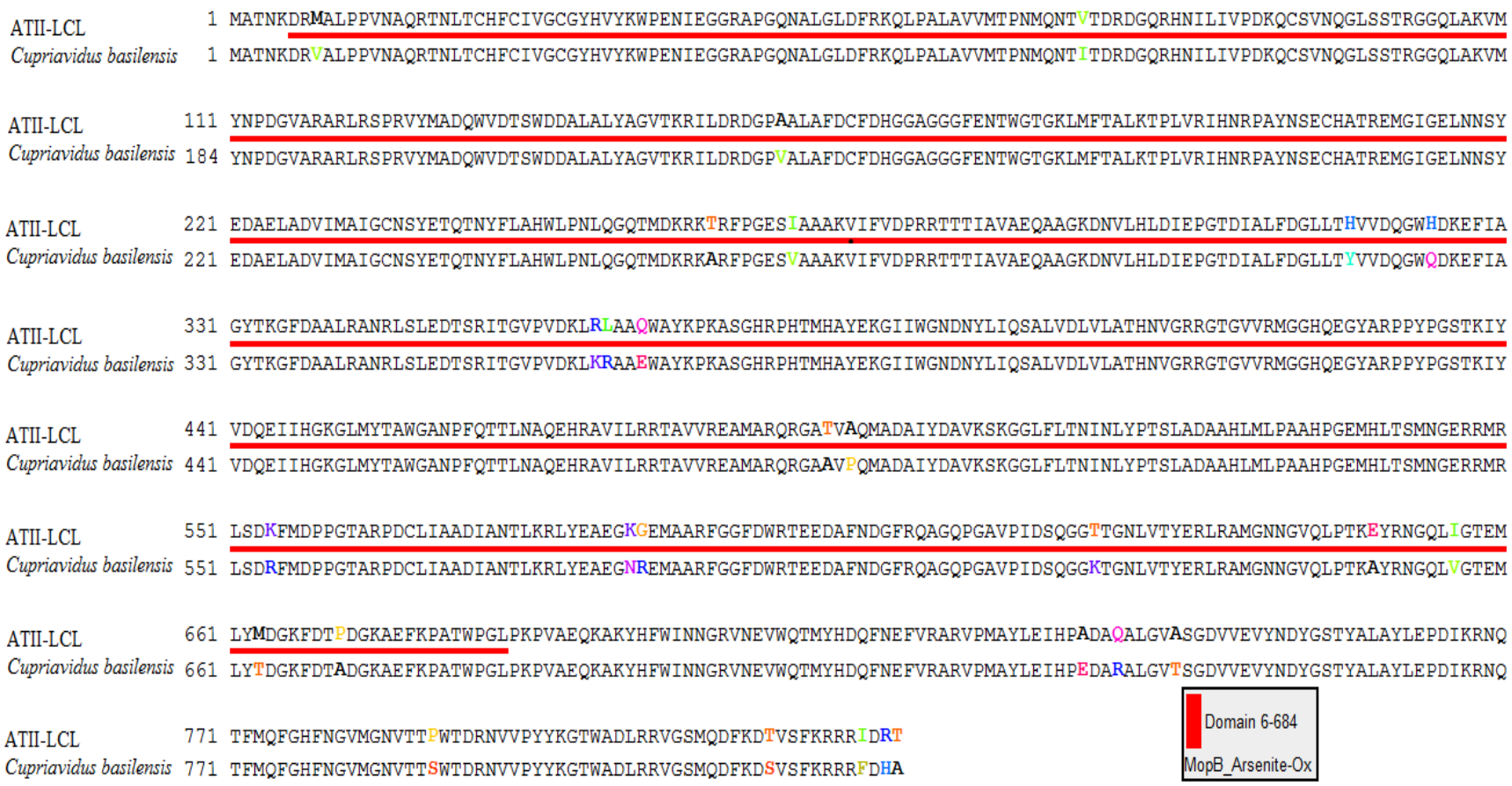

Figure 5. Sequence alignment between ATII-LCL ArOX and *Cupriavidus basilensis* ArOX large subunits by STRAP tool [86].

Molybdopterin binding conserved domain (MopB_Arsenite-Ox) is underlined in red (Accession: cd02756). BLASTx of ATII-LCL ArOX large subunit sequence against NR (Non-redundant) protein database showed 97% identity, 99 % query coverage, E-value =zero, and total score of 1646 with ArOX large subunit of *Cupriavidus basilensis* (Accession: WP_017228048.1).

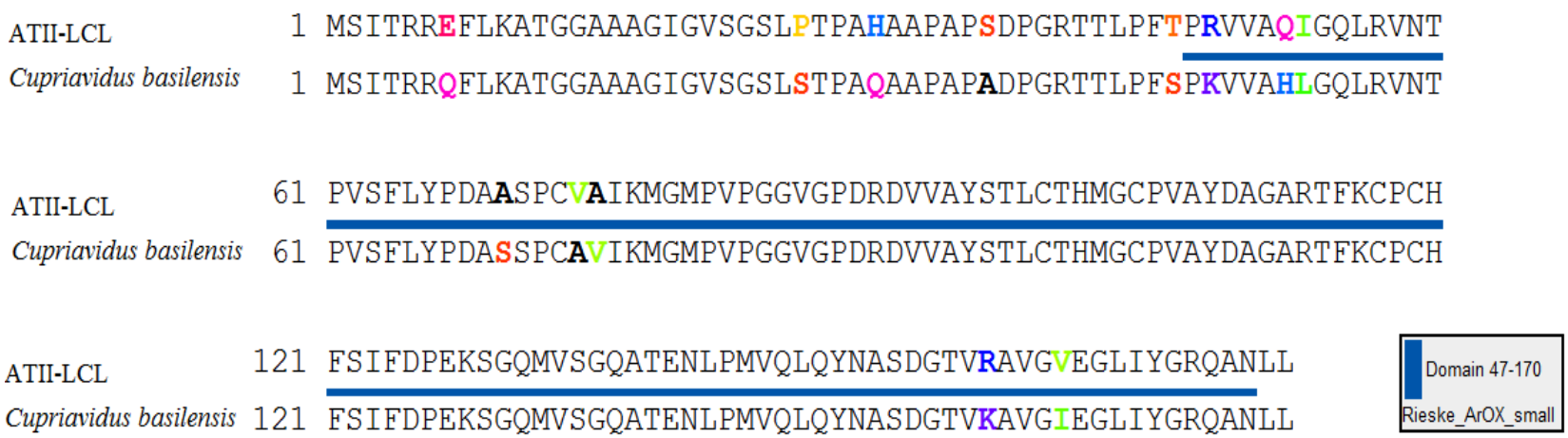

Figure 6. Sequence alignment between ATII-LCL ArOX and *Cupriavidus basilensis* ArOX small subunits by STRAP tool [86].

Rieske conserved domain (Rieske_ArOX_small) is underlined in blue (Accession: cd03476). BLASTx of ATII-LCL ArOX small subunit sequence against NR (Non-redundant) protein database showed 92% identity, 99 % query coverage, E-value = 1e-80 and total score of 248 with ArOX small subunit of *Cupriavidus basilensis* (Accession: WP_017228049.1).

8. Tables

Table 1. 16S rRNA pyrotag data sets of brine pools' water layers.

	ATII-LCL	ATII-UCL	DD	KD	Total
Bacterial 16S rRNA pyrotags	11,546	21,506	12,455	20,677	66,184
Archaeal 16S rRNA pyrotags	18,378	25,956	11,838	12,977	69,149
Unknown	67	139	775	255	1,236
Total 16S rRNA pyrotag reads	29,991	47,601	25,068	33,909	136,569

Table 2. Statistical data of metagenomic datasets of brine pools' water layers, computed by MG-RAST.

	ATII-LCL	ATII-UCL	DD	KD
Total number of sequences	1,143,149	660,692	669,512	1,139,639
Total number of basepairs	461,486,669	256,440,157	237,395,937	311,265,240
Average length of sequences (bps)	403	388	354	273
Number of sequences containing ribosomal RNA genes	29,725(2.6%)	17,000(2.6%)	11,941(1.8%)	15,170(1.3%)
Number of sequences containing predicted proteins with known functions	755,862(66.1%)	378,612(57.3%)	315,428(47.1%)	298,024(26.2%)
Number of sequences containing predicted proteins with unknown function	350,874(30.7%)	259,528(39.3%)	324,379(48.5%)	774,868(68.0%)
Number of sequences do not contain rRNA genes or predicted proteins	6,688(0.6%)	5,552 (0.8%)	17,764 (2.7%)	51,577(4.5%)

Table 3. Chemical profiling of brine pools' water samples in ppm.

	Rare metals and chemical elements (ppm)																			Highly abundant metals (ppm)			
	Al Aluminum	As Arsenic	Au Gold	B Boron	Ba Barium	Cu Copper	Fe Iron	Li Lithium	Mn Manganese	P Phosphorus	Pb Lead	Pt Platinum	Rb Rubidium	Ru Ruthenium	Si Silicon	Sn Tin	Sr Strontium	W Tungsten	Zn Zinc	Ca Calcium	K Potassium	Mg Magnesium	Na Sodium
ATII-LCL	0.1	0.1	1.9	8.8	1.9	0.1	47.6	3.5	78.9	0.1	0.1	0.5	0	0	5.1	0	45.6	0.1	3.9	5300	2700	1000	85400
DD	0.1	0.3	1.4	8.5	0.6	0	0.1	3.1	52.9	0.2	0	0	10.2	0	1.4	0	47.4	0.2	0.7	3200	1600	672	65100
KD	0.1	0.2	0.1	20.8	0.1	0	0.1	2.7	5.3	0.7	0	0.2	1.8	0.1	5.4	0.1	49.7	0.2	0.2	1500	1100	2500	94100

Table 4. Number of reads and relative abundance of peroxidases enzymes within PeroxiBase database in brine pools' water layers.

Peroxidases		ATII-LCL		ATII-UCL		DD		KD	
Non haem peroxidases	Thiol peroxidase: Glutathione peroxidase superfamily: Bacteria glutathione peroxidase (GPx)	203	0.018%	70	0.011%	12	0.002%	3	0.000%
	Manganese catalse family: Manganese Catalase (MnCat)	90	0.008%	35	0.005%	0	0.000%	0	0.000%
	Haloperoxidase superfamily : No haem, no metal haloperoxidase (HalNPrx)	61	0.005%	17	0.003%	8	0.001%	2	0.000%
	Alkylhydroperoxidase D-like superfamily: Carboxymuconolactone decarboxylase (peroxidase activity) (CMD)	50	0.004%	15	0.002%	5	0.001%	21	0.002%
	Thiol peroxidase: Peroxiredoxin superfamily: Atypical 2-Cysteine peroxiredoxin (BCP)	44	0.004%	20	0.003%	47	0.007%	2	0.000%
	Thiol peroxidase: Peroxiredoxin superfamily: 1-Cysteine peroxiredoxin (1CysPrx)	15	0.001%	2	0.000%	22	0.003%	11	0.001%
	Thiol peroxidase: Peroxiredoxin superfamily: AhpC like peroxiredoxin(AhpC)	14	0.001%	2	0.000%	9	0.001%	5	0.000%
	Thiol peroxidase: Peroxiredoxin superfamily: AhpE like peroxiredoxin (AhpE)	1	0.000%	0	0.000%	10	0.001%	0	0.000%
Haem peroxidases	Catalase family : Catalase (Kat)	250	0.022%	97	0.015%	3	0.000%	2	0.000%
	Di-haem peroxidase superfamily: Other di-haem peroxidase (DiHPOX)	89	0.008%	36	0.005%	2	0.000%	1	0.000%
	DyP-type peroxidase superfamily: DyP-type peroxidase A (DyPrx)	42	0.004%	13	0.002%	0	0.000%	0	0.000%
	Non Animal peroxidase: Class I peroxidase superfamily : Catalase peroxidase (CP)	35	0.003%	5	0.001%	40	0.006%	6	0.001%
	Peroxidase-Cyclooxygenase superfamily: PeroxinectinShort peroxidockerin (PxDo)	20	0.002%	7	0.001%	3	0.000%	0	0.000%
Total number of reads		914	0.080%	319	0.048%	161	0.024%	53	0.005%
nber of sequences in metagenome		1143149		660692		669512		1139639	

Table 5. Number of reads and relative abundance of metal resistance genes within SEED Subsystems database in brine pools' water layers.

	ATII-LCL		ATII-UCL		DD		KD	
Cobalt-zinc-cadmium resistance genes	7681	0.672%	2398	0.363%	448	0.067%	163	0.014%
Copper resistance genes	5400	0.472%	1852	0.280%	281	0.042%	335	0.029%
Mercuric resistance genes	898	0.079%	311	0.047%	264	0.039%	10	0.001%
Chromate resistance genes	221	0.019%	76	0.012%	1	0.000%	1	0.000%
Arsenic resistance genes	153	0.013%	34	0.005%	127	0.019%	63	0.006%
Total number of reads	14353	1.256%	4671	0.707%	1121	0.167%	572	0.050%
Total number of sequences in the metagenome	1143149		660692		669512		1139639	

Table 6. Number of reads and relative abundance of genes involved in iron transport and metabolism within SEED Subsystems database in brine pools' water layers.

	ATII-LCL		ATII-UCL		DD		KD	
Total number of reads	2259	0.198%	673	0.102%	306	0.046%	195	0.017%
Total number of sequences in the metagenome	1143149		660692		669512		1139639	

Table 7. Number of reads and relative abundance of genes involved in membrane transport of metals within SEED Subsystems database in brine pools' water layers.

	ATII-LCL		ATII-UCL		DD		KD	
Manganese transport	914	0.080%	321	0.049%	29	0.004%	5	0.000%
Zinc transport	473	0.041%	100	0.015%	62	0.009%	26	0.002%
Molybdenum transport	204	0.018%	75	0.011%	25	0.004%	18	0.002%
Nickel and Cobalt transport	50	0.004%	15	0.002%	3	0.000%	18	0.002%
Total number of reads	1641	0.144%	511	0.077%	119	0.018%	67	0.006%
Total number of sequences in the metagenome	1143149		660692		669512		1139639	

Table 8. Amino acids composition and number of salt bridges of both ATII-LCL and *Cupriavidus basilensis* arsenite oxidase subunits.

	LCL large subunit	*Cupriavidus basilensis* large subunit	LCL small subunit	*Cupriavidus basilensis* small subunit
Total number of residues	828	828	172	172
Negatively charge residues (Asp+Glu)	90	91	11	10
Positively charge residues (Arg +Lys)	93	95	13	13
Salt bridges	70	75	8	7

Supplementary Table 1. Taxonomic assignment and relative abundance of significant highly abundant (relative abundance ≥ 5%) and rare (5% ≤ relative abundance ≥1%) bacterial OTUs obtained from brine pools' water.

	No. of OTU Clusters	Domain	Phylum	Class	Order	Family	Genus/Last identified taxa	ATII-LCL		ATII-UCL		DD		KD	
Highly abundant OTUs (relative abundance ≥ 5%)	1	Bacteria	Firmicutes	Bacilli	Bacillales	Paenibacillaceae	Paenibacillus	7294	64.22%	0	0.00%	0	0.00%	0	0.00%
	7		Proteobacteria	Alphaproteobacteria	Rhizobiales	Phyllobacteriaceae	Phyllobacterium	21	0.18%	10737	53.96%	0	0.00%	0	0.00%
	5		Deferribacteres	Deferribacteres	Deferribacterales	SAR406	SAR406	0	0.00%	2032	10.21%	9	0.08%	1	0.01%
	4		Proteobacteria	Gammaproteobacteria	Pseudomonadales	Moraxellaceae	Enhydrobacter	0	0.00%	2660	13.37%	0	0.00%	0	0.00%
	2		Proteobacteria	Betaproteobacteria	Burkholderiales	Comamonadaceae	Acidovorax	3	0.03%	0	0.00%	0	0.00%	8582	44.07%
	1		Proteobacteria	Betaproteobacteria	Burkholderiales	Comamonadaceae	Roseateles	0	0.00%	0	0.00%	0	0.00%	5184	26.62%
	4		Proteobacteria	Gammaproteobacteria	Alteromonadales	Alteromonadaceae	Alteromonas	1781	15.68%	1	0.01%	803	6.79%	0	0.00%
	4		Proteobacteria	Gammaproteobacteria	Oceanospirillales	Halomonadaceae	Halomonas	118	1.04%	0	0.00%	5146	43.49%	0	0.00%
	4		Proteobacteria	Betaproteobacteria	Burkholderiales	Burkholderiaceae	Cupriavidus	280	2.47%	3245	16.31%	0	0.00%	518	2.66%
Rare OTUs (5% ≤ relative abundance ≥1%)	2	Bacteria	OP1	NA	NA	NA	OP1	0	0.00%	0	0.00%	3	0.03%	736	3.78%
	2		Proteobacteria	Alphaproteobacteria	Sphingomonadales	Sphingomonadaceae	Sphingomonas	0	0.00%	0	0.00%	0	0.00%	280	1.44%
	1		Proteobacteria	Betaproteobacteria	Burkholderiales	Comamonadaceae	Comamonadaceae	3	0.03%	0	0.00%	0	0.00%	208	1.07%
	1		Proteobacteria	Betaproteobacteria	Burkholderiales	Comamonadaceae	Aquabacterium	0	0.00%	0	0.00%	0	0.00%	357	1.83%
	1		Proteobacteria	Betaproteobacteria	Burkholderiales	Comamonadaceae	Delftia	8	0.07%	0	0.00%	0	0.00%	252	1.29%
	1		Proteobacteria	Betaproteobacteria	Rhodocyclales	Rhodocyclaceae	Dechloromonas	0	0.00%	0	0.00%	1	0.01%	414	2.13%
	2		Proteobacteria	Deltaproteobacteria	NA	NA	Deltaproteobacteria	0	0.00%	0	0.00%	1	0.01%	385	1.98%
	3		Proteobacteria	Deltaproteobacteria	Desulfovibrionales	Desulfohalobiaceae	Desulfovermiculus	0	0.00%	0	0.00%	14	0.12%	385	1.98%
	2		Proteobacteria	Gammaproteobacteria	Alteromonadales	Pseudoalteromonadaceae	Pseudoalteromonas	0	0.00%	0	0.00%	0	0.00%	514	2.64%
	5		Proteobacteria	Gammaproteobacteria	Pseudomonadales	Moraxellaceae	Acinetobacter	76	0.67%	0	0.00%	281	2.37%	327	1.68%
	3		Actinobacteria	Actinobacteria	Actinomycetales	NA	Actinomycetales	0	0.00%	23	0.12%	230	1.94%	0	0.00%
	1		Proteobacteria	Gammaproteobacteria	Pseudomonadales	Moraxellaceae	Psychrobacter	0	0.00%	0	0.00%	119	1.01%	0	0.00%
	1		Proteobacteria	Alphaproteobacteria	Rhodobacterales	Rhodobacteraceae	Loktanella	0	0.00%	0	0.00%	510	4.31%	0	0.00%
	1		Proteobacteria	Alphaproteobacteria	Rhodobacterales	Rhodobacteraceae	Sulfitobacter	0	0.00%	0	0.00%	371	3.14%	0	0.00%
	1		Proteobacteria	Alphaproteobacteria	Sphingomonadales	Erythrobacteraceae	Erythrobacter	2	0.02%	0	0.00%	366	3.09%	0	0.00%
	1		Proteobacteria	Alphaproteobacteria	Caulobacterales	Caulobacteraceae	Brevundimonas	139	1.22%	0	0.00%	0	0.00%	0	0.00%
	2		Proteobacteria	Gammaproteobacteria	Enterobacteriales	Enterobacteriaceae	Enterobacteriaceae	237	2.09%	0	0.00%	0	0.00%	0	0.00%
	1		Proteobacteria	Gammaproteobacteria	Pseudomonadales	Pseudomonadaceae	Pseudomonas	125	1.10%	1	0.01%	0	0.00%	3	0.02%
Total number of sequences clustered into OTUs								11358		19897		11832		19474	

Supplementary Table 2. Taxonomic assignment and relative abundance of significant highly abundant (relative abundance ≥ 5%) and rare (5% ≤ relative abundance ≥1%) archaeal OTUs obtained from brine pools' water.

	No. of OTU Clusters	Domain	Phylum	Class	Order	Family	Genus/Last identified taxa	ATII-LCL		ATII-UCL		DD		KD	
Highly abundant OTUs (relative abundance ≥ 5%)	4	Archaea	Crenarchaeota	Marine Group I	NA	NA	Marine Group I	2292	14.46%	16396	87.31%	4	0.04%	11	0.09%
	5		Euryarchaeota	Methanomicrobia	ST-12K10A	NA	ST-12K10A	0	0.00%	0	0.00%	2802	27.09%	14	0.12%
	7		Euryarchaeota	Halobacteria	Halobacteriales	Halobacteriaceae	Halobacteriaceae	0	0.00%	0	0.00%	1227	11.86%	0	0.00%
	44		Euryarchaeota	Thermoplasmata	South African Goldmine Group	NA	South African Goldmine Group	44	0.28%	103	0.55%	5166	49.95%	11202	95.78%
	9		Euryarchaeota	Thermoplasmata	Thermoplasmatales	Marine Group II	Marine Group II	3938	24.84%	0	0.00%	0	0.00%	0	0.00%
Rare OTUs (5% ≤ relative abundance ≥1%)	2	Archaea	Crenarchaeota	Terrestrial Hot Spring Group	NA	NA	Terrestrial Hot Spring Group	0	0.00%	0	0.00%	108	1.04%	0	0.00%
	3		Euryarchaeota	Halobacteria	Halobacteriales	Deep Sea Hydrothermal Vent Group 6	Deep Sea Hydrothermal Vent Group 6	35	0.22%	208	1.11%	0	0.00%	0	0.00%
	2		Euryarchaeota	Halobacteria	Halobacteriales	Halobacteriaceae	Halomicrobium	0	0.00%	0	0.00%	251	2.43%	0	0.00%
	1		Euryarchaeota	Halobacteria	Halobacteriales	MSP41	MSP41	0	0.00%	0	0.00%	167	1.61%	0	0.00%
	1		Euryarchaeota	Methanomicrobia	Methanosarcinales	Methanosaetaceae	Methanosaeta	619	3.90%	528	2.81%	0	0.00%	0	0.00%
	2		Euryarchaeota	Thermoplasmata	Marine Benthic Group E	NA	Marine Benthic Group E	709	4.47%	884	4.71%	3	0.03%	0	0.00%
Total number of sequences clustered into OTUs								15856		18778		10342		11695	

Supplementary Table 3. Metal resistance genes and their relative abundance within SEED Subsystems database in brine pools' water layers.

	ATII-LCL		ATII-UCL		DD		KD	
Arsenate reductase (EC 1.20.4.1)	95	0.008%	21	0.003%	19	0.003%	0	0.000%
Arsenic resistance protein ArsH	46	0.004%	9	0.001%	0	0.000%	0	0.000%
Arsenical-resistance protein ACR3	12	0.001%	4	0.001%	0	0.000%	63	0.006%
Blue copper oxidase CueO precursor	0	0.000%	0	0.000%	30	0.004%	0	0.000%
Cobalt-zinc-cadmium resistance protein CzcA	2375	0.208%	805	0.122%	107	0.016%	46	0.004%
Chromate resistance protein ChrB	38	0.003%	9	0.001%	1	0.000%	0	0.000%
Chromate transport protein ChrA	137	0.012%	58	0.009%	0	0.000%	0	0.000%
Cobalt/zinc/cadmium efflux RND transporter, membrane fusion protein, CzcB family	614	0.054%	188	0.028%	6	0.001%	10	0.001%
Cobalt-zinc-cadmium resistance protein	2821	0.247%	925	0.140%	59	0.009%	70	0.006%
Cobalt-zinc-cadmium resistance protein CzcD	215	0.019%	51	0.008%	7	0.001%	8	0.001%
CopG protein	197	0.017%	23	0.003%	6	0.001%	3	0.000%
Copper-binding periplasmic protein	0	0.000%	0	0.000%	10	0.001%	0	0.000%
Copper-sensing two-component system response regulator CusR	248	0.022%	100	0.015%	0	0.000%	2	0.000%
Copper-translocating P-type ATPase (EC 3.6.3.4)	2074	0.181%	676	0.102%	66	0.010%	312	0.027%
Copper chaperone	23	0.002%	12	0.002%	0	0.000%	0	0.000%
Copper homeostasis protein CutE	64	0.006%	12	0.002%	26	0.004%	0	0.000%
Copper resistance protein B	781	0.068%	234	0.035%	0	0.000%	0	0.000%
Copper resistance protein C precursor	169	0.015%	75	0.011%	0	0.000%	0	0.000%
Copper resistance protein D	464	0.041%	155	0.023%	10	0.001%	0	0.000%
Copper sensory histidine kinase CusS	184	0.016%	110	0.017%	1	0.000%	4	0.000%
Copper tolerance protein	64	0.006%	58	0.009%	0	0.000%	3	0.000%
Cytochrome c heme lyase subunit CcmF	65	0.006%	20	0.003%	34	0.005%	0	0.000%
Cytochrome c heme lyase subunit CcmH	18	0.002%	7	0.001%	4	0.001%	0	0.000%
DNA-binding heavy metal response regulator	344	0.030%	85	0.013%	10	0.001%	7	0.001%
Heavy metal resistance transcriptional regulator HmrR	5	0.000%	2	0.000%	10	0.001%	0	0.000%
Heavy metal RND efflux outer membrane protein, CzcC family	456	0.040%	141	0.021%	14	0.002%	0	0.000%
Heavy metal sensor histidine kinase	530	0.046%	67	0.010%	12	0.002%	5	0.000%
Magnesium and cobalt efflux protein CorC	39	0.003%	14	0.002%	20	0.003%	4	0.000%
Mercuric ion reductase (EC 1.16.1.1)	279	0.024%	121	0.018%	5	0.001%	8	0.001%
Mercuric resistance operon coregulator	89	0.008%	14	0.002%	0	0.000%	0	0.000%
Mercuric resistance operon regulatory protein	218	0.019%	44	0.007%	73	0.011%	1	0.000%
Mercuric transport protein, MerC	2	0.000%	0	0.000%	34	0.005%	0	0.000%
Mercuric transport protein, MerE	26	0.002%	18	0.003%	31	0.005%	0	0.000%
Mercuric transport protein, MerT	136	0.012%	51	0.008%	0	0.000%	1	0.000%
Multicopper oxidase	1049	0.092%	370	0.056%	55	0.008%	11	0.001%
Periplasmic mercury(+2) binding protein	81	0.007%	43	0.007%	33	0.005%	0	0.000%
PF00070 family, FAD-dependent NAD(P)-disulphide oxidoreductase	67	0.006%	20	0.003%	88	0.013%	0	0.000%
Probable cadmium-transporting ATPase (EC 3.6.3.3)	0	0.000%	0	0.000%	24	0.004%	0	0.000%
Probable Co/Zn/Cd efflux system membrane fusion protein	216	0.019%	92	0.014%	72	0.011%	6	0.001%
Putative copper efflux system protein CusB	0	0.000%	0	0.000%	39	0.006%	0	0.000%
Putative silver efflux pump	0	0.000%	0	0.000%	32	0.005%	0	0.000%
Respiratory arsenate reductase, Mo binding subunit (ArrA)	0	0.000%	0	0.000%	38	0.006%	0	0.000%
Respiratory arsentate reductase, FeS subunit (ArrB)	0	0.000%	0	0.000%	70	0.010%	0	0.000%
Response regulator of zinc sigma-54-dependent two-component system	12	0.001%	9	0.001%	27	0.004%	3	0.000%
Superoxide dismutase SodM-like protein ChrF	46	0.004%	9	0.001%	0	0.000%	1	0.000%
Transcriptional regulator, MerR family	48	0.004%	18	0.003%	8	0.001%	4	0.000%
Zinc transporter ZitB	6	0.001%	1	0.000%	23	0.003%	0	0.000%
Zn(II) and Co(II) transmembrane diffusion facilitator	0	0.000%	0	0.000%	17	0.003%	0	0.000%
Total number of reads	14353	1.256%	4671	0.707%	1121	0.167%	572	0.050%
Total number of sequences in the metagenome	1143149		660692		669512		1139639	

Supplementary Table 4. Metal resistance genes and their relative abundance within BacMet database (experimentally confirmed resistance genes) in brine pools' water layers.

	ATII-LCL		ATII-UCL		DD		KD	
Molybdate/tungstate import ATP-binding protein WtpC	757	0.066%	240	0.036%	119	0.018%	184	0.016%
Copper-transporting P-type ATPase	488	0.043%	207	0.031%	14	0.002%	24	0.002%
Putative cation efflux system protein SilA	446	0.039%	188	0.028%	16	0.002%	6	0.001%
Copper resistance protein A	425	0.037%	175	0.026%	4	0.001%	4	0.000%
Fe(3+) ions import ATP-binding protein FbpC 2	391	0.034%	181	0.027%	112	0.017%	51	0.004%
Cation efflux system protein CusA	349	0.031%	136	0.021%	9	0.001%	5	0.000%
Nickel import ATP-binding protein NikD	346	0.030%	139	0.021%	49	0.007%	31	0.003%
Multidrug resistance protein MdtB -Zinc (Zn)	327	0.029%	115	0.017%	7	0.001%	6	0.001%
Nickel import ATP-binding protein NikE	319	0.028%	116	0.018%	70	0.010%	25	0.002%
Copper resistance protein B	293	0.026%	122	0.018%	1	0.000%	0	0.000%
Lead uptake protein PbrT	289	0.025%	110	0.017%	1	0.000%	5	0.000%
Nickel transport system permease protein NikB	284	0.025%	100	0.015%	33	0.005%	24	0.002%
Multidrug resistance protein MdtC -Zinc (Zn)	270	0.024%	95	0.014%	5	0.001%	7	0.001%
Putative cation efflux system protein	262	0.023%	107	0.016%	9	0.001%	8	0.001%
Silver exporting P-type ATPase	248	0.022%	98	0.015%	17	0.003%	8	0.001%
CopJ protein	229	0.020%	81	0.012%	4	0.001%	0	0.000%
Zinc import ATP-binding protein ZnuC	206	0.018%	95	0.014%	75	0.011%	89	0.008%
CzcP cation efflux P1-ATPase	197	0.017%	76	0.012%	1	0.000%	22	0.002%
Nickel and cobalt resistance protein CnrA	197	0.017%	88	0.013%	2	0.000%	1	0.000%
Cobalt-zinc-cadmium resistance protein CzcA	187	0.016%	90	0.014%	11	0.002%	12	0.001%
Copper resistance protein K	181	0.016%	87	0.013%	0	0.000%	1	0.000%
Nickel transport system permease protein NikC	178	0.016%	70	0.011%	30	0.004%	16	0.001%
MerA	171	0.015%	73	0.011%	8	0.001%	15	0.001%
Sensor kinase CusS	154	0.013%	57	0.009%	0	0.000%	4	0.000%
Transcriptional regulatory protein CusR	150	0.013%	62	0.009%	0	0.000%	3	0.000%
Transcriptional activator protein CopR	148	0.013%	51	0.008%	7	0.001%	6	0.001%
CopR	136	0.012%	52	0.008%	12	0.002%	21	0.002%
NcrA	136	0.012%	61	0.009%	2	0.000%	1	0.000%
CopD	131	0.011%	48	0.007%	0	0.000%	0	0.000%
Nickel-cobalt-cadmium resistance protein NccA	130	0.011%	65	0.010%	1	0.000%	1	0.000%
P-type ATPase involved in Pb(II) resistance PbrA	130	0.011%	45	0.007%	0	0.000%	55	0.005%
Probable copper-exporting P-type ATPase V	122	0.011%	37	0.006%	4	0.001%	30	0.003%
Copper resistance protein C	121	0.011%	42	0.006%	0	0.000%	0	0.000%
Copper resistance protein D	117	0.010%	38	0.006%	0	0.000%	0	0.000%
Inner membrane ABC-transporter YbtQ -Iron (Fe)	117	0.010%	47	0.007%	66	0.010%	31	0.003%
CzcE, involved in Cd(II), Zn(II), Co(II) resistance	114	0.010%	36	0.005%	0	0.000%	0	0.000%
CmeB -Copper (Cu), Cobalt (Co)	103	0.009%	45	0.007%	7	0.001%	4	0.000%
Sensor protein CzcS	100	0.009%	37	0.006%	0	0.000%	0	0.000%
Transcriptional regulatory protein ZraR -Zinc (Zn)	99	0.009%	34	0.005%	52	0.008%	11	0.001%
MerR	95	0.008%	28	0.004%	1	0.000%	7	0.001%
Transcriptional regulatory protein PmrA -Iron (Fe)	95	0.008%	39	0.006%	1	0.000%	2	0.000%
Multidrug resistance protein MdtA -Zinc (Zn)	90	0.008%	44	0.007%	0	0.000%	3	0.000%
Cation efflux system protein CusB	88	0.008%	27	0.004%	0	0.000%	2	0.000%
CopA	88	0.008%	46	0.007%	3	0.000%	1	0.000%
Cobalt-zinc-cadmium resistance protein CzcD	74	0.006%	27	0.004%	1	0.000%	7	0.001%
Aconitate hydratase - Iron (Fe)	73	0.006%	39	0.006%	65	0.010%	7	0.001%
Molybdenum import ATP-binding protein ModC	72	0.006%	32	0.005%	21	0.003%	23	0.002%
Lipoprotein signal peptidase -Lead (Pb)	68	0.006%	30	0.005%	10	0.001%	4	0.000%
Copper transporter	67	0.006%	25	0.004%	4	0.001%	5	0.000%
Chaperone protein DnaK -Copper (Cu)	65	0.006%	33	0.005%	119	0.018%	63	0.006%
Holliday junction ATP-dependent DNA helicase RuvB -Chromium (Cr), Tellurium (Te), Selenium (Se)	65	0.006%	18	0.003%	48	0.007%	19	0.002%

Supplementary Table 4. ***(continued)*** **Metal resistance genes and their relative abundance within BacMet database (experimentally confirmed resistance genes) in brine pools' water layers.**

	ATII-LCL		ATII-UCL		DD		KD	
Transcriptional activator protein CzcR	65	0.006%	32	0.005%	4	0.001%	8	0.001%
Sensor protein ZraS -Zinc (Zn)	64	0.006%	17	0.003%	25	0.004%	10	0.001%
Sigma-54 dependent DNA-binding response regulator -Copper (Cu)	64	0.006%	36	0.005%	35	0.005%	10	0.001%
Cobalt-zinc-cadmium resistance protein CzcB	63	0.006%	37	0.006%	0	0.000%	3	0.000%
Nickel and cobalt resistance protein CnrB	62	0.005%	27	0.004%	0	0.000%	0	0.000%
HupE2 -Nickel (Ni)	61	0.005%	25	0.004%	0	0.000%	0	0.000%
Uncharacterized ABC transporter ATP-binding protein YbbL- Iron (Fe)	60	0.005%	23	0.003%	16	0.002%	17	0.001%
Acid tolerance regulatory protein ActR- Cadmium (Cd), Zinc (Zn)	57	0.005%	26	0.004%	9	0.001%	2	0.000%
CopS	55	0.005%	28	0.004%	0	0.000%	4	0.000%
Probable transcriptional regulatory protein SilR	55	0.005%	11	0.002%	2	0.000%	1	0.000%
SitB -Manganese (Mn), Iron (Fe)	53	0.005%	17	0.003%	6	0.001%	39	0.003%
ChrF	49	0.004%	13	0.002%	0	0.000%	1	0.000%
Nickel-binding periplasmic protein	49	0.004%	9	0.001%	3	0.000%	7	0.001%
MerD from Tn4378, regulatory protein involved in Hg(II) resistance	47	0.004%	13	0.002%	0	0.000%	0	0.000%
Low-affinity inorganic phosphate transporter 1 -Zinc (Zn), Tellurium (Te)	45	0.004%	9	0.001%	3	0.000%	2	0.000%
SitC -Manganese (Mn), Iron (Fe)	44	0.004%	14	0.002%	0	0.000%	0	0.000%
Superoxide dismutase [Fe]	44	0.004%	11	0.002%	3	0.000%	4	0.000%
MerT	43	0.004%	18	0.003%	0	0.000%	0	0.000%
Molybdenum transport system permease protein ModB	42	0.004%	15	0.002%	6	0.001%	2	0.000%
Transcriptional regulatory protein BaeR -Zinc (Zn), Tungsten (W)	42	0.004%	8	0.001%	5	0.001%	1	0.000%
Cobalt-zinc-cadmium resistance protein CzcC	41	0.004%	14	0.002%	2	0.000%	5	0.000%
Arsenic resistance protein ArsH	39	0.003%	10	0.002%	0	0.000%	0	0.000%
Arsenate reductase	38	0.003%	10	0.002%	5	0.001%	7	0.001%
HTH-type transcriptional repressor ComR -Copper (Cu)	37	0.003%	12	0.002%	0	0.000%	1	0.000%
Apolipoprotein N-acyltransferase -Copper (Cu), Zinc (Zn)	36	0.003%	11	0.002%	11	0.002%	0	0.000%
Arsenite oxidase subunit AioA	36	0.003%	18	0.003%	1	0.000%	0	0.000%
Periplasmic chelated iron-binding protein YfeA	36	0.003%	4	0.001%	0	0.000%	1	0.000%
Chromate transporter	35	0.003%	17	0.003%	0	0.000%	1	0.000%
HTH-type transcriptional regulator ZntR	35	0.003%	9	0.001%	0	0.000%	0	0.000%
Putative cation efflux pump	35	0.003%	29	0.004%	1	0.000%	0	0.000%
CnrT, Cation Diffusion Facilitator, involved in Co(II), Ni(II) resistance	33	0.003%	13	0.002%	1	0.000%	2	0.000%
Iron transport protein, periplasmic-binding protein	33	0.003%	16	0.002%	0	0.000%	0	0.000%
Transcriptional activator protein IrlR- Cadmium (Cd), Zinc (Zn)	33	0.003%	16	0.002%	4	0.001%	2	0.000%
Chromate transport protein	32	0.003%	20	0.003%	0	0.000%	0	0.000%
Nickel-cobalt-cadmium resistance protein NccB	31	0.003%	9	0.001%	1	0.000%	0	0.000%
Phosphate-binding protein PstS -Arsenic (As)	31	0.003%	17	0.003%	0	0.000%	0	0.000%
Putative cation transport ATPase	31	0.003%	12	0.002%	4	0.001%	3	0.000%
PbrD, Pb(II) binding protein involved in Pb(II) resistance	30	0.003%	11	0.002%	0	0.000%	0	0.000%
MerP	29	0.003%	18	0.003%	0	0.000%	0	0.000%
Protein ChrB	28	0.002%	6	0.001%	0	0.000%	0	0.000%
Transcriptional regulatory protein PcoR -Copper (Cu)	28	0.002%	13	0.002%	3	0.000%	1	0.000%

Supplementary Table 4. ***(continued)*** **Metal resistance genes and their relative abundance within BacMet database (experimentally confirmed resistance genes) in brine pools' water layers.**

	ATII-LCL		ATII-UCL		DD		KD	
NirA	27	0.002%	9	0.001%	0	0.000%	0	0.000%
Uncharacterized mercuric resistance protein MerE	27	0.002%	12	0.002%	0	0.000%	0	0.000%
Magnesium-transporting ATPase, P-type 1	25	0.002%	11	0.002%	8	0.001%	87	0.008%
NcrB	25	0.002%	5	0.001%	0	0.000%	0	0.000%
Pb-specific transcription regulator protein	25	0.002%	7	0.001%	1	0.000%	3	0.000%
SitD -Manganese (Mn), Iron (Fe)	23	0.002%	10	0.002%	0	0.000%	1	0.000%
Nickel-cobalt-cadmium resistance protein NccN	22	0.002%	9	0.001%	0	0.000%	0	0.000%
Divalent metal cation transporter MntH -Manganese (Mn), Iron (Fe), Cadmium (Cd), Cobalt (Co), Zinc (Zn)	21	0.002%	6	0.001%	0	0.000%	1	0.000%
Molybdate/tungstate transport system permease protein WtpB	21	0.002%	6	0.001%	2	0.000%	40	0.004%
CopC	19	0.002%	21	0.003%	0	0.000%	0	0.000%
Copper-exporting P-type ATPase B	17	0.001%	4	0.001%	4	0.001%	162	0.014%
Copper-transporting ATPase	17	0.001%	2	0.000%	2	0.000%	0	0.000%
Cation or drug efflux system protein- Nickel (Ni)	12	0.001%	5	0.001%	23	0.003%	4	0.000%
Probable sensor protein PcoS -Copper (Cu)	6	0.001%	11	0.002%	2	0.000%	0	0.000%
Arsenite resistance protein ArsB	5	0.000%	2	0.000%	0	0.000%	31	0.003%
Cation-transporting ATPase E1-E2 ATPase -Cobalt (Co)	4	0.000%	0	0.000%	0	0.000%	24	0.002%
Superoxide dismutase [Mn]	3	0.000%	1	0.000%	20	0.003%	1	0.000%
Arsenical pump-driving ATPase	2	0.000%	0	0.000%	6	0.001%	40	0.004%
Mercuric resistance protein	2	0.000%	0	0.000%	16	0.002%	0	0.000%
Molybdate/tungstate-binding protein WtpA	2	0.000%	0	0.000%	0	0.000%	52	0.005%
Transcriptional regulator MntR -Manganese (Mn), Magnesium (Mg)	1	0.000%	1	0.000%	0	0.000%	19	0.002%
ArsP -arsenic resistance membrane permease	0	0.000%	0	0.000%	0	0.000%	19	0.002%
Zinc transporter ZupT	0	0.000%	0	0.000%	0	0.000%	16	0.001%
Total number of reads	12065	1.055%	4730	0.716%	1255	0.187%	1488	0.131%
Total number of sequences in the metagenome	1143149		660692		669512		1139639	

Supplementary Table 5. Genes involved in iron transport and metabolism and their relative abundance within SEED Subsystems database in brine pools' water layers.

	ATII-LCL		ATII-UCL		DD		KD	
ABC Fe3+ siderophore transporter, inner membrane subunit	2	0.000%	1	0.000%	31	0.005%	0	0.000%
ABC-type hemin transport system, ATPase component	19	0.002%	1	0.000%	3	0.000%	0	0.000%
ABC-type spermidine/putrescine transport systems, ATPase components	143	0.013%	40	0.006%	7	0.001%	0	0.000%
Bacterioferritin	23	0.002%	10	0.002%	7	0.001%	2	0.000%
Electron transfer flavoprotein, beta subunit	99	0.009%	24	0.004%	31	0.005%	31	0.003%
Ferric hydroxamate ABC transporter (TC 3.A.1.14.3), ATP-binding protein FhuC	17	0.001%	7	0.001%	2	0.000%	0	0.000%
Ferric hydroxamate ABC transporter (TC 3.A.1.14.3), permease component FhuB	24	0.002%	8	0.001%	0	0.000%	0	0.000%
Ferric iron ABC transporter, ATP-binding protein	123	0.011%	24	0.004%	16	0.002%	9	0.001%
Ferric iron ABC transporter, iron-binding protein	171	0.015%	52	0.008%	22	0.003%	0	0.000%
Ferric iron ABC transporter, permease protein	170	0.015%	44	0.007%	30	0.004%	4	0.000%
Ferrichrome transport ATP-binding protein FhuC (TC 3.A.1.14.3)	23	0.002%	3	0.000%	0	0.000%	0	0.000%
Ferrichrome-iron receptor	322	0.028%	91	0.014%	8	0.001%	13	0.001%
Ferrous iron transport periplasmic protein EfeO, contains peptidase-M75 domain and (frequently) cupredoxin-like domain	50	0.004%	16	0.002%	0	0.000%	0	0.000%
Ferrous iron transport permease EfeU	23	0.002%	15	0.002%	0	0.000%	0	0.000%
Ferrous iron transport peroxidase EfeB	52	0.005%	14	0.002%	0	0.000%	0	0.000%
Ferrous iron transport protein B	24	0.002%	10	0.002%	9	0.001%	98	0.009%
FIG039061: hypothetical protein related to heme utilization	27	0.002%	5	0.001%	0	0.000%	0	0.000%
Heme oxygenase HemO, associated with heme uptake	0	0.000%	0	0.000%	26	0.004%	0	0.000%
Heme-degrading monooxygenase IsdG (EC 1.14.99.3)	18	0.002%	1	0.000%	1	0.000%	0	0.000%
Hemin ABC transporter, permease protein	77	0.007%	14	0.002%	1	0.000%	0	0.000%
Hemin transport protein	40	0.003%	19	0.003%	0	0.000%	1	0.000%
Hemin transport protein HmuS	40	0.003%	19	0.003%	0	0.000%	0	0.000%
Hemin uptake protein	21	0.002%	5	0.001%	0	0.000%	1	0.000%
Iron-responsive regulator Irr	26	0.002%	8	0.001%	0	0.000%	0	0.000%
Iron-responsive repressor RirA	16	0.001%	9	0.001%	0	0.000%	0	0.000%
Iron-uptake factor PiuB	47	0.004%	20	0.003%	1	0.000%	1	0.000%
L-lysine 6-monooxygenase [NADPH] (EC 1.14.13.59), aerobactin biosynthesis protein IucD	38	0.003%	14	0.002%	0	0.000%	0	0.000%
L-ornithine 5-monooxygenase (EC 1.13.12.-), PvdA of pyoverdin biosynthesis	33	0.003%	5	0.001%	0	0.000%	0	0.000%
Outer membrane receptor proteins, likely involved in siderophore uptake	40	0.003%	8	0.001%	0	0.000%	0	0.000%
Paraquat-inducible protein A	26	0.002%	7	0.001%	1	0.000%	0	0.000%
Paraquat-inducible protein B	39	0.003%	12	0.002%	1	0.000%	0	0.000%
Periplasmic hemin-binding protein	33	0.003%	19	0.003%	0	0.000%	0	0.000%
Probable Lysine n(6)-hydroxylase associated with siderophore S biosynthesis (EC 1.14.13.59)	0	0.000%	0	0.000%	11	0.002%	0	0.000%
Putative high-affinity iron permease	165	0.014%	80	0.012%	0	0.000%	0	0.000%
Siderophore biosynthesis non-ribosomal peptide synthetase modules	61	0.005%	24	0.004%	2	0.000%	0	0.000%
Siderophore biosynthesis protein, monooxygenase	42	0.004%	13	0.002%	1	0.000%	0	0.000%
Siderophore synthetase small component, acetyltransferase	30	0.003%	3	0.000%	0	0.000%	0	0.000%
TonB-dependent hemin , ferrichrome receptor	16	0.001%	0	0.000%	0	0.000%	0	0.000%
TonB-dependent receptor	139	0.012%	28	0.004%	95	0.014%	35	0.003%
Total number of reads	2259	0.198%	673	0.102%	306	0.046%	195	0.017%
Total number of sequences in the metagenome	1143149		660692		669512		1139639	

Supplementary Table 6. Genes involved in membrane transport of metals and their relative abundance within SEED Subsystems database in brine pools' water layers.

	ATII-LCL		ATII-UCL		DD		KD	
HupE-UreJ family metal transporter	31	0.003%	12	0.002%	0	0.000%	0	0.000%
Manganese ABC transporter, ATP-binding protein SitB	63	0.006%	27	0.004%	6	0.001%	0	0.000%
Manganese ABC transporter, inner membrane permease protein SitC	65	0.006%	12	0.002%	7	0.001%	0	0.000%
Manganese ABC transporter, inner membrane permease protein SitD	42	0.004%	11	0.002%	16	0.002%	2	0.000%
Manganese ABC transporter, periplasmic-binding protein SitA	89	0.008%	25	0.004%	0	0.000%	0	0.000%
Manganese transport protein MntH	604	0.053%	214	0.032%	0	0.000%	3	0.000%
Manganese uptake regulation protein MUR	51	0.004%	32	0.005%	0	0.000%	0	0.000%
Molybdate-binding domain of ModE	28	0.002%	11	0.002%	0	0.000%	4	0.000%
Molybdenum ABC transporter, periplasmic molybdenum-binding protein ModA (TC 3.A.1.8.1)	28	0.002%	10	0.002%	7	0.001%	0	0.000%
Molybdenum transport ATP-binding protein ModC (TC 3.A.1.8.1)	94	0.008%	32	0.005%	8	0.001%	0	0.000%
Molybdenum transport system permease protein ModB (TC 3.A.1.8.1)	54	0.005%	22	0.003%	10	0.001%	14	0.001%
Nickel responsive regulator NikR	0	0.000%	0	0.000%	0	0.000%	18	0.002%
Predicted cobalt transporter CbtA	19	0.002%	3	0.000%	3	0.000%	0	0.000%
Putative metal chaperone, involved in Zn homeostasis, GTPase of COG0523 family	273	0.024%	65	0.010%	7	0.001%	5	0.000%
Zinc ABC transporter, ATP-binding protein ZnuC	58	0.005%	11	0.002%	11	0.002%	12	0.001%
Zinc ABC transporter, inner membrane permease protein ZnuB	44	0.004%	8	0.001%	10	0.001%	3	0.000%
Zinc ABC transporter, periplasmic-binding protein ZnuA	21	0.002%	6	0.001%	2	0.000%	0	0.000%
Zinc uptake regulation protein ZUR	29	0.003%	0	0.000%	6	0.001%	0	0.000%
Zinc-regulated outer membrane receptor	48	0.004%	10	0.002%	1	0.000%	6	0.001%
Zinc-regulated TonB-dependent outer membrane receptor	0	0.000%	0	0.000%	25	0.004%	0	0.000%
Total number of reads	1641	0.144%	511	0.077%	119	0.018%	67	0.006%
Total number of sequences in the metagenome	1143149		660692		669512		1139639	